Consistent fluctuations in intermediate water temperature off the coast of Greenland and Norway during Dansgaard-Oeschger events

E.G. Sessford [a], M.F. Jensen [a], A.A. Tisserand [b], F. Muschitiello [c, b], T. Dokken [b], K.H. Nisancioglu [a, d], E. Jansen [a, b, *]

[a] Department of Earth Science, University of Bergen, Bjerknes Centre for Climate Research, Allégaten 41, 5007, Bergen, Norway
[b] NORCE Norwegian Research Centre AS, Bjerknes Centre for Climate Research, Jahnebakken 5, 5007, Bergen, Norway
[c] University of Cambridge, Department of Geography, Downing Place, CB2 3EN, Cambridge, United Kingdom
[d] Centre for Earth Evolution and Dynamics, University of Oslo, Oslo, Norway

ARTICLE INFO

ABSTRACT

Rapid warmings epitomize the Dansgaard-Oeschger events that are recorded in Greenland ice cores and imprinted in ocean sediment cores. While the abrupt climate changes appear connected to perturbations in sea ice and ocean circulation, it is unclear how the water masses within the Nordic Seas responded and were influenced by the inflowing Atlantic Water in the absence or presence of sea ice. High resolution reconstructions of benthic Mg/Ca, together with stable isotopes of carbon and oxygen ($\delta^{13}C$ and $\delta^{18}O$), show a recurring warming ($2.5° \pm 0.5 °C$) occurring consistently at the inflow and outflow of the Nordic Seas at intermediate depths down to 1500 m during Greenland Stadials 9−6. Using idealized numerical simulations with an eddy-resolving ocean model we investigate the impact of an isolating sea ice cover and freshwater lid in the Nordic Seas. With the presence of an extensive sea ice cover, the warm Atlantic Water entering the Nordic Seas in the east, retains its heat as it exits in the west. The depth of the recirculating warm Atlantic Water increases when including an external freshwater source at the surface of the Nordic Seas. These findings support the view that cold stadials are accompanied by pervasive intermediate water warming across the Nordic Seas. Given the current rates of Arctic sea ice loss, these results provide a potential mechanism for water-column destabilization and inception of abrupt climate change.

© 2019 The Authors. Published by Elsevier Ltd. This is an open access article under the CC BY-NC-ND license (http://creativecommons.org/licenses/by-nc-nd/4.0/).

1. Introduction

Repeated episodes of rapid surface air temperature warming of 10−15 °C on Greenland punctuate the ice core records during the last glacial period, and in particular Marine Isotope Stage 3 (MIS3) 59 - 29 ka BP (Johnsen et al., 2001; Voelker, 2002). These events, commonly known as Dansgaard-Oeschger (D-O) events, were initially identified in stable isotope records from two Greenland ice cores (Dansgaard et al., 1993). Large in amplitude and abruptness, D-O events as seen in the Greenland ice cores exemplify a climatic system that rapidly switches between two quasi-stable states. The prevailing structure of a full event being rapid warmings that culminate within a few decades into Greenland Interstadial states

lasting about 200−400 years, followed by a gradual cooling (lasting approx. 50−200 years) succeeded by an abrupt drop into a cold Greenland Stadial period lasting approximately 200−2000 years (Dansgaard et al., 1993). These dramatic events have global implications as either temperature or precipitation events, as reflected in Greenland ice cores, marine sediment records and speleothem data (Wang et al., 2001; Rahmstorf, 2002; Voelker, 2002; Dokken et al., 2013; Buizert et al., 2015; Voelker and Haflidason, 2015).

In the North Atlantic and Nordic Seas, climate reconstructions from sediment cores record large variations in surface hydrographic conditions between Greenland Stadial and Greenland Interstadial periods such as, sea ice changes (Hoff et al., 2016; Wary et al., 2017a), sea surface and near surface temperature changes (Hall et al., 2011; Dokken et al., 2013), and movements of ocean fronts (Rasmussen et al., 2016). The millennial scale climate variability of the D-O events was originally attributed to changes in the rate or location of convection within the Nordic Seas/North Atlantic, thereby affecting the Atlantic Meridional Overturning Circulation

(AMOC) (Broecker et al., 1985; Menviel et al., 2014). The mechanisms responsible for shifts in AMOC are not fully understood. A number of modelling studies suggest a variety of potential mechanisms such as; Northern Hemisphere ice sheet topography (Zhang et al., 2014a), meltwater release (Zhang et al., 2015), gradual changes in atmospheric CO_2 (Zhang et al., 2017) and wind driven forcing (Krebs and Timmermann, 2007; Kleppin et al., 2015). However, the leading hypotheses implicate ocean driven changes that are regulated by a combination of a Nordic Seas ice cover and strong halocline made up of a cold and fresh surface layer above more salty waters (Dokken and Jansen, 1999; Elliot et al., 2001; Shaffer et al., 2004; Li et al., 2010; Dokken et al., 2013; Petersen et al., 2013; Ezat et al., 2014; Bassis et al., 2017). High-resolution records of D-O variability with respect to surface water and sea ice conditions in the Nordic Seas are forthcoming (Dokken et al., 2013; Voelker and Haflidason, 2015; Rasmussen et al., 2016; Wary et al., 2017b; Sadatzki et al., 2019), including improved chronologies tied to the Greenland ice cores. However, the potential changes to intermediate and deep waters in the Nordic Seas and their positioning within the abrupt D-O events are not well known and have been limited by the low resolution of available sediment records (Marcott et al., 2011; Ezat et al., 2014). Here we explore both sides of the Nordic Seas basin in high-resolution marine records as well as an eddy resolving ocean circulation model to document the response of intermediate water masses during abrupt D-O events.

Shifts in the location of the sea ice edge have been proposed as a main component regulating the D-O cycles, their amplitude and abruptness (Gildor and Tziperman, 2003; Dokken et al., 2013) because of its strong impact on regional climate and potential to respond quickly to weak changes in atmospheric or oceanic forcing (Li et al., 2010; Masson-Delmotte et al., 2013; Petersen et al., 2013). The majority of studies relate cold atmospheric temperatures and stadial periods to expanding sea ice conditions; and the opposite for interstadial periods. Multiple studies have attempted to reconstruct past Nordic Seas parameters using indirect proxies from Greenland ice cores and ocean sediment cores to understand the changes in sea ice variability. For example, ice core records of bromine enrichment from Renland indicate changes in first year sea ice growth over the last 120 kys, and thereby reciprocate movement of the sea ice edge between 50 and 85°N (Maffezzoli et al., 2018). Redistribution of water masses within the water column, as reconstructed through proxy records from high-resolution ocean sediment cores, indicate changes in sea ice conditions (Dokken et al., 2013; Wary et al., 2017b; Sadatzki et al., 2019). Benthic $\delta^{18}O$ records have been implemented to argue for the influence of brine release and thereby the formation of sea ice during stadial periods (Dokken and Jansen, 1999; Dokken et al., 2013). Other studies use more direct proxies for sea ice reconstruction such as the marine biomarker IP_{25} (Hoff et al., 2016; Sadatzki et al., 2019). Marine biomarker reconstructions and benthic $\delta^{18}O$ records (Vidal et al., 1998; van Kreveld et al., 2000; Hagen and Hald, 2002) indicate that during Greenland Stadials there is extensive sea ice cover over the Nordic Seas and south of the Greenland-Scotland Ridge, but common for these is a relatively low temporal resolution in comparison with ice core records. During Greenland Interstadials the sea ice retreats some distance into the Nordic Seas allowing for open water vertical mixing. In contrast to this popular scheme, dinoflagellate cyst records are interpreted to indicate the presence of sea ice in the Nordic Seas associated with Greenland Interstadials and open ocean convection associated with Greenland Stadials (Eynaud et al., 2002; Wary et al., 2015; Wary et al., 2016; Wary et al., 2017a; Wary et al., 2017b). However, proxy studies of intermediate water in the Nordic Seas and North Atlantic do not support this scheme (Vidal et al., 1998; van Kreveld et al., 2000; Hagen and Hald, 2002; Rasmussen and Thomsen, 2004; Marcott

et al., 2011; Ezat et al., 2014).

In the eastern Nordic Seas margin, benthic assemblages (Rasmussen and Thomsen, 2004) and Mg/Ca reconstructions (Ezat et al., 2014) are used to identify Atlantic Water intrusion at intermediate depth during Greenland Stadials. In the western Nordic Seas margin, species specific benthic Mg/Ca reconstructions from *Cassidulina neoteretis* (herein referred to as Mg/Ca_{CN}) indicate increased intermediate warming during stadials (Sessford et al., 2018). Sub-surface warming under well stratified water conditions in the North Atlantic has mostly been studied for Heinrich Events, however some of the same mechanisms may apply for stadial conditions. Marcott et al. (2011) use a combination of benthic Mg/Ca reconstructions and climate model simulations that reveal North Atlantic basin wide intermediate water warming during Heinrich Events that coincide with large reductions in AMOC.

Jensen et al. (2018) investigated the sensitivity of a Nordic Sea ice cover to the temperature of the Atlantic inflow using an eddy-resolving general circulation model. The authors found a threshold where sea ice responds non-linearly to small changes in Atlantic Water temperature. At low Atlantic Water temperatures (<4 °C) the Nordic Seas is fully covered in sea ice, while the boundaries are free of sea ice for warm Atlantic Water (>4.5 °C). The two different sea ice states give markedly different hydrographies across the Nordic Seas, and changes in the depth of the Atlantic Water. When the boundaries are free of sea ice, the Atlantic Water inflow is found at the surface. The warm water cools as it circulates the Nordic Seas, and the eastern side is ~4 °C warmer than the west. Under sea ice covered conditions, the warm Atlantic Water is found at depth isolated from the atmosphere and sea ice by a cold fresh surface layer. In this case, the Atlantic Water retains its heat as it circulates in the Nordic Seas, and the same water mass properties are found at the Norwegian and Greenland margins of the basin. The latter state is associated with Greenland Stadials with extensive sea ice cover.

Results from Sessford et al., (2018) agree with this scheme. They produced a high-resolution benthic Mg/Ca_{CN} record from the Denmark Strait indicating intermediate water temperatures of 2.5 ± 1 °C during Greenland Stadials and 0.5 ± 1 °C for Greenland Interstadials. These authors rely on calculating the stable oxygen composition of ocean water as an indirect proxy of brine intrusion and thereby sea ice production. In lack of direct sea ice proxy measurements from the area, these are the only published indications of sea ice for the Denmark Strait during D-O events. To investigate if warm intermediate water of Atlantic origin is circulating the Nordic Seas beneath the sea ice during Greenland Stadials intermediate water records from both sides of the basin are required. Ezat et al. (2014) produced a combined high-resolution Mg/Ca record of benthic foraminifera measured on *C. neoteretis* and *M. barleeanum* in the eastern Nordic Seas to show low amplitude variation in intermediate water temperature between Greenland Interstadials, 1 ± 0.5 °C and Greenland Stadials, 2 ± 0.5 °C. However, the time period between 40−33 ka, covered by our study is mainly comprised of *M. barleeanum* and only of eight *C. neoteretis* measurements in the Ezat et al. (2014) data set. Furthermore, the less aggressive oxidative cleaning method used in Ezat et al., (2014) might over-estimate the Mg concentrations in foraminifera shells, specifically in the lower end of the spectrum, and is not logical to use here as all of the available temperature calibrations have been made using the reductive cleaning method (Kristjánsdóttir et al., 2007; Barrientos et al., 2018; Sessford et al., 2018). To directly compare and reduce uncertainties as a result of using different species for temperature reconstruction, and, to potentially capture the lower end of the temperature spectrum better, the intermediate water temperatures between the inflow

and outflow regions of the Nordic Seas are measured in this study using the same species as in Sessford et al. (2018), *C. neoteretis*.

In this study we present new proxy and climate model evidence in support of a consistent intermediate water warming across the Nordic Seas during Greenland Stadial events, suggesting that heat in the Atlantic layer is retained by the presence of extensive sea ice and a halocline in the Nordic Seas. Our proxy reconstructions are based on novel and published Mg/Ca$_{CN}$ measurements of benthic foraminifera from the Faroe-Shetland Rise and the northern Denmark Strait, respectively. We attempt to reconstruct past circulation between the Nordic Seas and the North Atlantic using a combination of new intermediate water temperature records, published proxy records (Table 1) and additional model simulations to those of Jensen et al. (2018).

2. Oceanographic setting

The Nordic Seas are separated from the North Atlantic by the Greenland-Scotland Ridge which forms a barrier at 840 m depth (Hansen and Østerhus, 2000). This ridge is divided up into three channels that allow for the movement of water between the basins. In the present interglacial, and of interest for the last glacial period, water mass exchange between the North Atlantic and the Nordic Seas flows through two main channels; the Faroe-Shetland Channel in the east as the primary inflow channel and the Denmark Strait in the west as the main outflow channel (Fig. 1) (Hansen and Østerhus, 2000). Because the proxy and modelling methods in this study are not able to distinguish between all the potential water masses entering and exiting the Nordic Seas, we use the interpretations of Våge et al. (2013) and Hansen and Østerhus, (2000) while discussing our results.

Northward surface flow of warm (>7 °C) Atlantic Water enters the Nordic Seas down to ≈ 500 m as the Northern Icelandic Irminger Current in the Denmark Strait on the western margin of the Nordic Seas and the North Atlantic Current through the Faroe-Shetland Channel at the eastern margin (Hansen and Østerhus, 2000). The dominant inflow into the Nordic Seas is through the Faroe-Shetland Channel whereas the dominant overflow (outflow) is through the Denmark Strait. The amount of overflow water exiting the Nordic Seas in modern times is approximately 6 Sv in the Denmark Strait (3 Sv as Polar Surface Water (PSW) and 3 Sv as

intermediate/deep water) and approximately 1.5 Sv in the Faroe-Shetland Channel (Hansen and Østerhus, 2000). Intermediate and deep water make up the return flow of cold, dense Denmark Strait Overflow Water (DSOW) and Iceland-Scotland Overflow Water (ISOW) to the North Atlantic.

The DSOW is formed by a variety of water masses (Tanhua et al., 2005; Jeansson et al., 2008). However, it is generally thought that Atlantic Originating Water (Atl), having circulated through the Nordic Seas, forms the major part of the overflow as intermediate water (Våge et al., 2013). Atl is made up of modified Atlantic Water (>0 °C) formed by mixing in the Norwegian Sea and Fram Strait (Våge et al., 2011; Våge et al., 2013). Colder DSOW (<0 °C) is considered to be made up of Arctic Originating Water as described by Våge et al., (2011; 2013) which is mainly formed by convection of the Northern Icelandic Irminger Current in the Iceland Sea Gyre. The rest of the Denmark Strait outflow is cold, fresh, PSW as part of the East Greenland Current and often contains sea ice and ice bergs (Jeansson et al., 2008).

The ISOW contains two water masses; an intermediate water mass mainly formed in the Norwegian Sea (Norwegian Sea Arctic Intermediate Water, NSAIW) through convection that generally does not sink to depths greater than 1000 m; and Norwegian Sea Deep Water (NSDW) (Hansen and Østerhus, 2000). Temperatures of NSAIW are between −0.5 and + 0.5 °C. These waters form either through deep convection, or on shallow shelf regions through the formation of sea ice and brine rejection (Hansen and Østerhus, 2000; Ullgren et al., 2016). The NSDW has a temperature of less than −0.5 °C and is mostly formed during winter, when sea ice production is more predominant (Hansen and Østerhus, 2000). In order for NSDW to spill into the North Atlantic it must ascend above the sill level through vertical mixing (Hansen and Østerhus, 2000). The remaining NSDW, that does not ascend above the sill depth, contributes to water in the deep Nordic Seas becoming old, stagnant and depleted in δ^{13}C (Sarnthein et al., 1994). Because of sea floor ridges dividing the Nordic Seas basins the ISOW is capable of entraining old NSDW from the deep basins, whereas the DSOW cannot (Rudels and Quadfasel, 1991; Hansen and Østerhus, 2000).

Table 1

Core name, type of proxy and reference to cited work used in discussion and Fig. 7. Proxy subscripts refer to the species or method used for the proxy records. Species: C. neoteretis −.CN; M. barleeanum −.Mb; N. pachyderma − NP; Cibicides lobatulus − Cl; Cibicides wuellerstorfi − Cw; Transfer functions: SIMMAX Modern analogue technique − MAT; Maximum likelihood − ML; Weighed Average Partial Least-Squares − WAPLS; Back propagation Artificial Neural Network − ANN.

| Label in Fig. 1	Core	Types of data implemented	Time interval (ka)	Reference
1	MD99-2284	Benthic Mg/Ca$_{CN}$	33−39	This Study
	MD99-2284	Planktic $\delta^{18}O_{NP}$, $\delta^{13}C_{NP}$, δ_w, %NP, SST$_{ML}$, IRD Benthic $\delta^{18}O_{CN}$, $\delta^{13}C_{CN}$	31−42	(Dokken et al., 2013)
	MD99-2284	P$_B$IP$_{25}$		(Sadatzki et al., 2019)
2	JM11-FI-19PC	P$_B$IP$_{25}$	0−90	(Hoff et al., 2016)
	JM11-FI-19PC	Benthic Mg/Ca$_{CN\ and\ Mb}$	0−64	(Ezat et al., 2014)
3	MD99-2285	Dinoflagellate Cysts SIC and SST, IRD	35−41	(Wary et al., 2016)
4	ENAM93-21	Planktic $\delta^{18}O_{NP}$, $\delta^{13}C_{NP}$, %NP Benthic $\delta^{18}O_{Cl}$, $\delta^{13}C_{Cl}$, IRD, assemblage counts	0−140	(Rasmussen and Thomsen, 2004, 2009)
5	GS15-198-36CC	Benthic Mg/Ca$_{CN}$, $\delta^{18}O_{CN}$, $\delta^{13}C_{CN}$, δ_w	31−39	(Sessford et al., 2018)
6	PS2644-5	Planktic $\delta^{18}O_{NP}$, $\delta^{13}C_{NP}$, IRD, %NP, NP concentrations	0−80	(Voelker et al., 2000; Voelker and Haflidason, 2015)
7	JM96-1225	Benthic $\delta^{18}O_{Cw}$, $\delta^{13}C_{Cw}$, SST$_{MAT}$	0−55	(Hagen and Hald, 2002)
8	SO82-5	Planktic $\delta^{18}O_{NP}$, $\delta^{13}C_{NP}$ Benthic $\delta^{18}O_{Cw}$, $\delta^{13}C_{Cw}$, SST$_{MAT}$, IRD	18−60	(van Kreveld et al., 2000)
9	LO09-18	SST$_{NP}$, IRD	31−47	(Jonkers et al., 2010)
10	SO82-02GGC	SST$_{WAPLS}$, IRD	20−60	(Rasmussen et al., 2016)
11	V29-202	Benthic $\delta^{18}O_{Cw}$, $\delta^{13}C_{Cw}$	0−60	(Vidal et al., 1998)
12	NA87-22			
13	MD04-2829CQ	Planktic $\delta^{18}O_{NP}$, SST$_{ANN}$, %NP, IRD	18−41	(Hall et al., 2011)
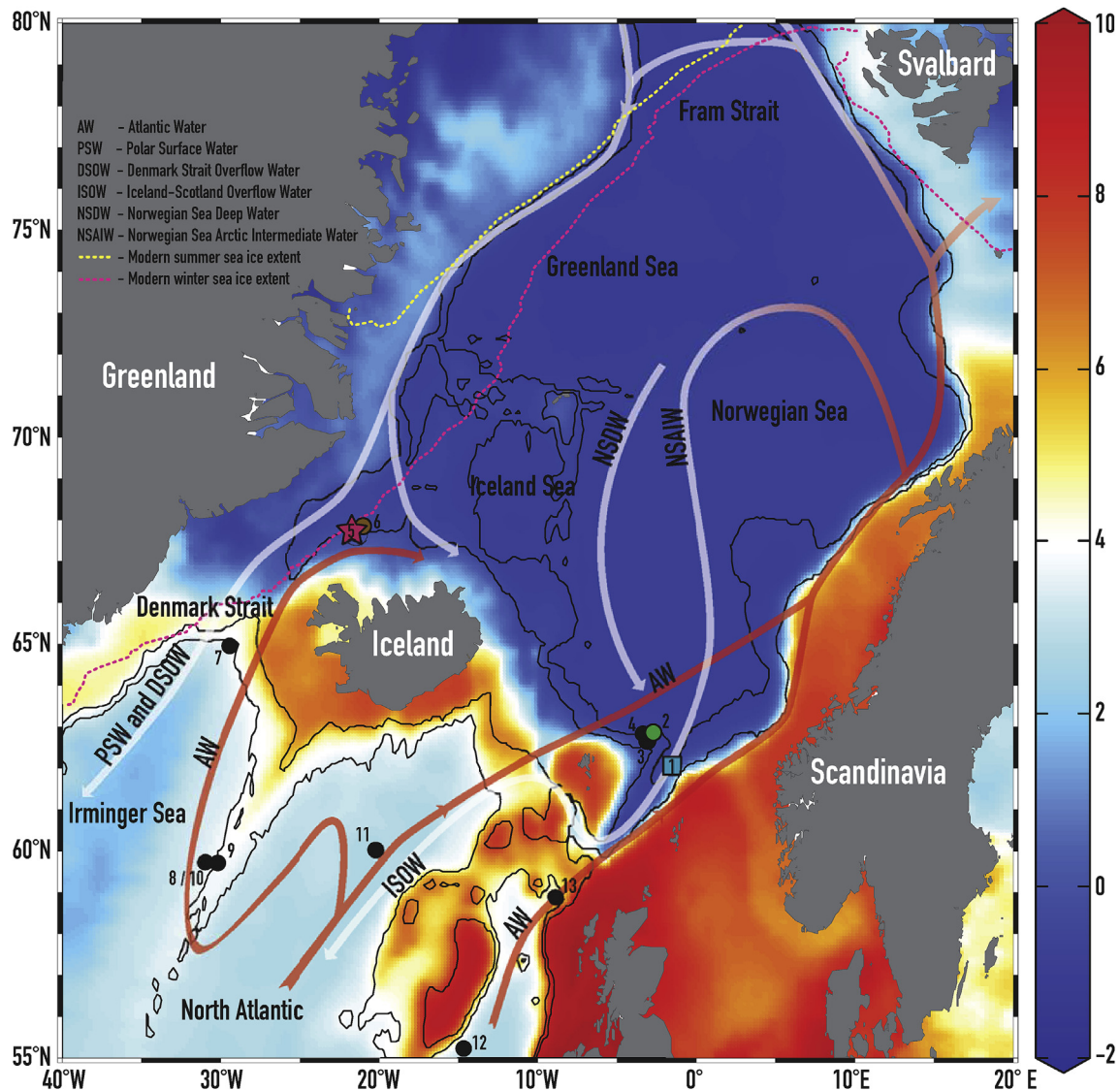
Fig. 1. Map of the study area highlighting modern temperatures in °C at the sea floor and showing locations of the sediment cores on corresponding depth isoline: MD99-2284 with a blue square [1] on the 1500 m isoline, GS15-198-36CC with a pink star [5] on the 750 m isoline. Supporting records used in figures from published data at sites JM11-FI-19PC (Hoff et al., 2016) and PS2644-5 (Voelker and Haflidason, 2015) in green [2] and brown circles [6], respectively. Supporting records from the North Atlantic and Nordic Seas discussed and used to support circulation schematics in Fig. 7 are shown as black dots, core number corresponds to Table 1. Dotted lines indicate modern sea ice extent for March (pink) and September (yellow) averaged between A.D. 1981 and 2010 (Fetterer et al., 2017, updated daily). Thick dashed red line indicates the approximate location of the transect as shown in the model in Fig. 4b and c. Figure created in part with Ocean Data View (Schlitzer, 2014) and GLODAP v2 data (Olsen et al., 2016).

3. Materials and methods

3.1. Core sites

In this study we present new benthic Mg/Ca$_{CN}$ data from core MD99-2284 from the Faroe-Shetland Rise (62°22′ N, 0°58′ W, 1500 m) (Fig. 1), which allow tracking paleoceanographic changes in the eastern Nordic Seas.

These are combined with published data from two cores located in the Denmark Strait and Western Nordic Seas, i.e. cores PS2644-5 (67°52′ N, 21°45′ W, water depth 777 m) (Voelker et al., 1998) and GS15-198-36CC (67°51′ N, 21°52′ W, water depth 770 m) (Sessford et al., 2018) (Fig. 1). We exploit the ice rafted debris (IRD) counts, *Neoglobiquadrina pachyderma* (NP) (N. pachyderma strictly refers to sinistral forms of the species (Darling et al., 2006; Eynaud et al., 2009), counts and δ^{18}O$_{NP}$ stable isotopes from PS2644-5 to discuss the surface water conditions of the western sector of the

Nordic Seas. GS15-198-36CC measurements of Mg/Ca$_{CN}$ and derived intermediate water temperature (IWT), stable isotopes (δ^{18}O$_{CN}$ and δ^{13}C$_{CN}$) and stable isotope composition of water (δ$_w$) of benthic species *Cassidulina neoteretis* (CN) are used for intermediate water conditions.

3.2. Proxy reconstructions of temperature and water mass properties

We refer the reader to Sessford et al., (2018) for method details concerning sampling and data measurement practices for core GS15-198-36CC and to Voelker (2002) and Voelker and Haflidison (2015) for methods concerning core PS2644-5. For P$_B$IP$_{25}$ sea ice reconstruction methods we refer the reader to Hoff et al. (2016) for JM11-FI-19PC and Sadatzki et al. (2019) for MD99-2284. The reader is referred to the methods section of Dokken et al. (2013) for further details concerning data from core MD99-2284 and measurements
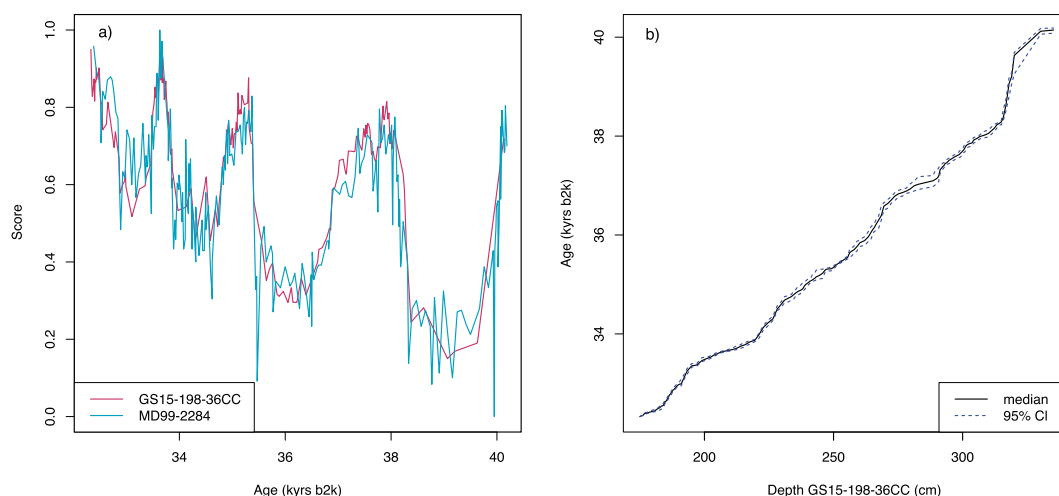
Fig. 2. Age-depth model of core GS15-198-36CC based on synchronization to MD99-2284 using benthic $\delta^{18}O_{CN}$. Synchronization was obtained via a Markov Chain Monte Carlo (MCMC) proxy series alignment method (Muschitiello et al., 2015a; 2015b) (see text for details). a) Optimal (median) placement of GS15-198-36CC benthic $\delta^{18}O_{CN}$ onto the MD99-2284 benthic $\delta^{18}O_{CN}$ stratigraphy after 10^6 MCMC iterations. Time series were pre-normalized to be between 0 and 1 prior to synchronization. b) Age-depth mapping function of GS15-198-36CC benthic $\delta^{18}O_{CN}$ onto the MD99-2284 timescale, together with Monte Carlo 95% confidence levels.

of stable isotopes (*N. pachyderma* and *C. neoteretis*), calculated near sea-surface temperatures based on transfer functions of planktonic foraminifera, and calculations of stable oxygen composition of ocean water for the upper water column from *N. pachyderma*. Intermediate water temperatures and stable oxygen composition of bottom water (δ_w) are new measurements from this study and methods are discussed below.

MD99-2284 has been extensively sampled in the past and very little material is left; measured samples are therefore not at regular intervals. The majority of *C. neoteretis* samples picked for Mg/Ca$_{CN}$ runs are from 1 cm slices, however where *C. neoteretis* abundance was too low 2, 3, 5 and 10 cm were combined together in 12, 3, 1 and 1 samples, respectively. The resulting resolution is decadal to centennial. Only pristine shells of *C. neoteretis* in the size fraction 150−500 μm, were gently crushed between two glass plates under a microscope to allow visual contaminants to be removed, homogenized, and then cleaned and analyzed for Mg/Ca$_{CN}$, Paired isotope − Mg/Ca$_{CN}$ was not possible due to lack of material; however, isotope analysis was conducted on all sample depths (Dokken et al., 2013). On average 90 pristine specimens were used for trace element analyses.

Trace element analysis samples were cleaned following the procedure described by Boyle and Keigwin, (1985/86) and Barker et al., (2003). This included clay removal, a reductive step to remove metal-oxide coatings, an oxidative step to remove organic matter, and a weak acid leaching step to remove absorbed contaminants. All samples were dissolved in trace metal pure 0.1 M HNO_3 and diluted to a final concentration of 40 ppm of calcium. Trace elements were measured at the Trace Element Lab (TELab) at NORCE, Bergen (Norway) on an Agilent 720 inductively coupled plasma optical emission spectrometer (ICP-OES) against standards with matched calcium concentration to reduce matrix effects (Rosenthal et al., 1999). Six in-house standards have been prepared at TELab and have a composition similar to foraminiferal carbonate (0.5−7.66 mmol/mol^{-1}). Long-term Mg/Ca$_{CN}$ analytical precision is ±0.020 mmol mol^{-1} (1σ standard deviation) or 0.39% (relative standard deviation) based on replicate analyses of a standard solution containing Mg/Ca$_{CN}$ ratios of 5.076 mmol mol^{-1} and a Ca concentration of 40 ppm. The average Mg/Ca of long-term international limestone standard (ECRM752-1) measurements is 3.76 mmol mol^{-1} (1σ = 0.07 mmol mol^{-1}) with the average

published value of 3.75 mmol mol^{-1} (Greaves et al., 2008).

Contamination-screening steps have been undertaken to monitor possible contamination by clays and/or Ferro-Manganese-oxide coatings. These steps consist on evaluating the correlations between Mg/Ca$_{CN}$ ratios with contaminant ratios, as Fe/Ca$_{CN}$, Al/Ca$_{CN}$ and Mn/Ca$_{CN}$ along the downcore results. The regression analysis and the coefficient of determination, R^2, explaining the variance between Mg/Ca$_{CN}$ and Fe/Ca$_{CN}$, Al/Ca$_{CN}$ and Mn/Ca$_{CN}$, are 0.34, 0.01, and 0.06, respectively, indicating no systematic contamination due to insufficient cleaning for manganese, Mn and aluminium, Al, however there is potential for low contamination by iron, Fe. The average downcore measurements for Fe/Ca$_{CN}$, Al/Ca$_{CN}$ and Mn/Ca$_{CN}$ analyses in *C. neoteretis* are 143 μmol/mol, 441 μmol/mol, and 145 μmol/mol, respectively (Supplementary data). All elements are close to the suggested contamination limits, 100 μmol/mol (Fe/Ca) and 400 μmol/mol (Al/Ca) (Barker et al., 2003; Skirbekk et al., 2016; Barrientos et al., 2018) and 105 μmol/mol (Mn/Ca) (Boyle, 1983). The elevated correlation between Fe/Ca$_{CN}$ and Mg/Ca$_{CN}$ suggests that the mechanisms controlling the concentration of iron and magnesium into the foraminiferal tests could be related and must be taken into consideration when we discuss temperature reconstructions in the following discussion. Following burial processes, Fe-Mn metal oxide may coat the tests and can result in anomalously high Mg/Ca of foraminiferal (Barker et al., 2003; Barker et al., 2005; Ferguson et al., 2008; Pena et al., 2008; Hönisch et al., 2013; Hasenfratz et al., 2017). However, the correlation between Mn/Ca$_{CN}$ and Mg/Ca$_{CN}$ is very low indicating that our results are unlikely affected by diagenetic coatings.

Conversion of the Mg/Ca$_{CN}$ values to IWT was done using the species-specific calibration equation for *C. neoteretis*;

$$Mg/Ca = (0.763(\pm0.05) * \exp(0.111(\pm0.02)*IWT \quad r2 = 0.90 \tag{1}$$

with a standard error of the estimate to be ±0.84 °C (Sessford et al., 2018). A 2σ temperature error (95% Confidence Level) of the calibration equation, combined with the analytical error, results in temperature uncertainty of measured Mg/Ca$_{CN}$ in core MD99-2284 to be ±1 °C for the temperature range (−0.89 °C − 4.55 °C) (Supplementary data).

To calculate the stable oxygen composition of ocean water (δ_w), oxygen isotope based temperature estimates are generated using
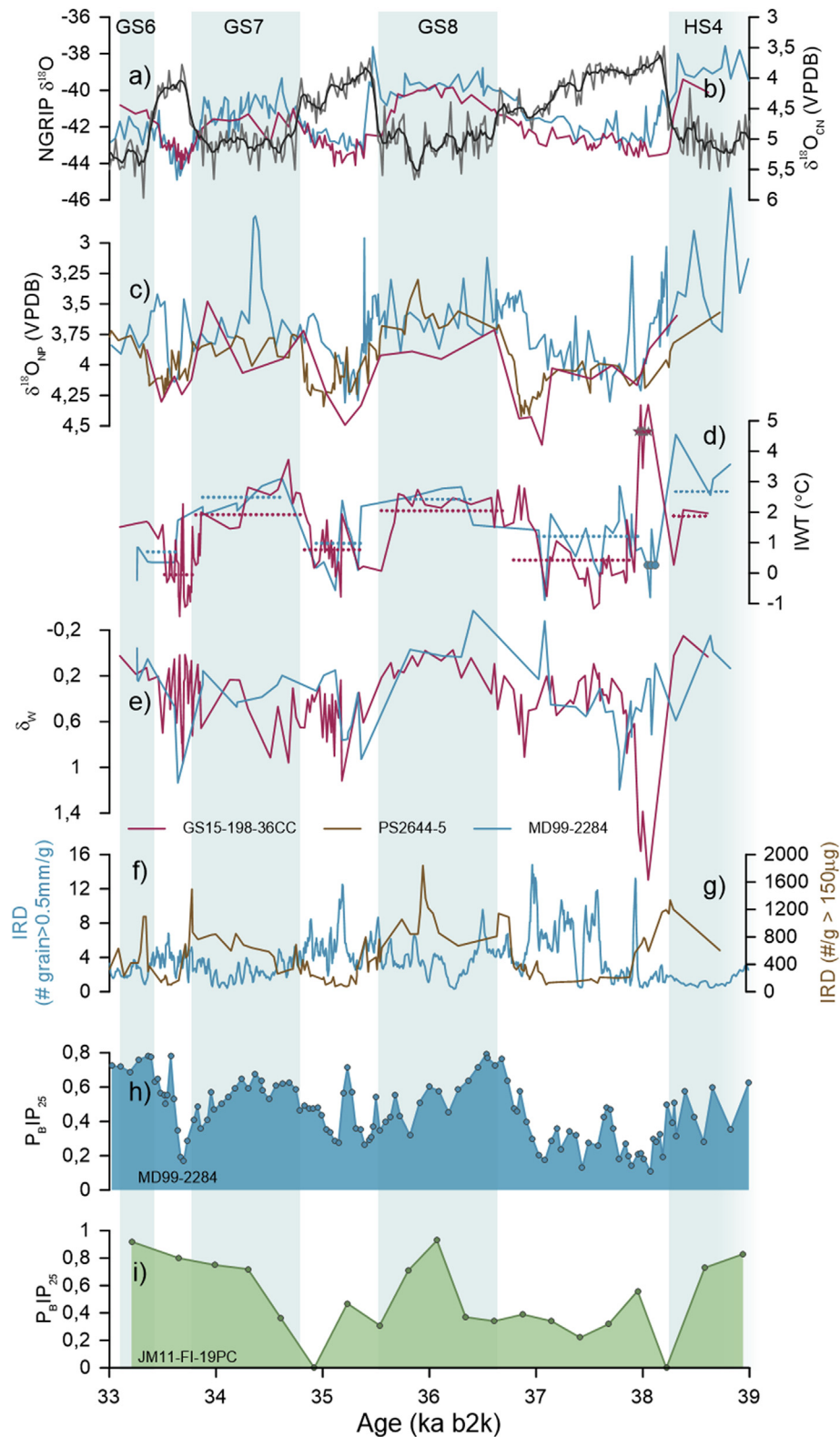
Fig. 3. Downcore reconstructions of D-O events 8−6 and part of Heinrich Stadial 4 (HS4) highlighting the consistent fluctuations in intermediate water hydrography between the Denmark Strait and the Faroe-Shetland Channel as associated with variations in sea ice records from the Norwegian Sea. Core GS15-198-36CC is identified as a pink line, PS2644-5 as a brown line and MD99-2284 as a blue line. Interstadial − Mode B periods are denoted with white bars. Stadial − Mode A, periods are denoted with blue shading and are defined by the transitions in a) NGRIP δ18O. The plots are as follows: b) benthic δ18O of C. neoteretis; c) δ18O of N. pachyderma; (d) intermediate water temperature as derived from Mg/Ca on the benthic species, C. neoteretis − dotted lines indicate the average temperatures for each period, with stars and circles indicating the Mode C, only occurring after Heinrich Stadial 4; e) stable oxygen composition of ocean water as calculated from C. neoteretis f) ice rafted debris counts from MD99-2284; g) ice rafted debris counts from PS2644-5 (Voelker et al., 2000)and; independent sea ice proxies from two sediment cores in the eastern Nordic Seas highlighting the similarities between h) P_BIP_{25} from MD99-2284 (Sadatzki et al., 2019) using the age model in this study and i) P_BIP_{25} from JM11-FI-19PC using the original age model from Hoff et al. (2016). See Table 1 for an overview of the cores and data and associated authors. Interstadial event following HS4 − Mode C, is highlighted with diagonal bars.
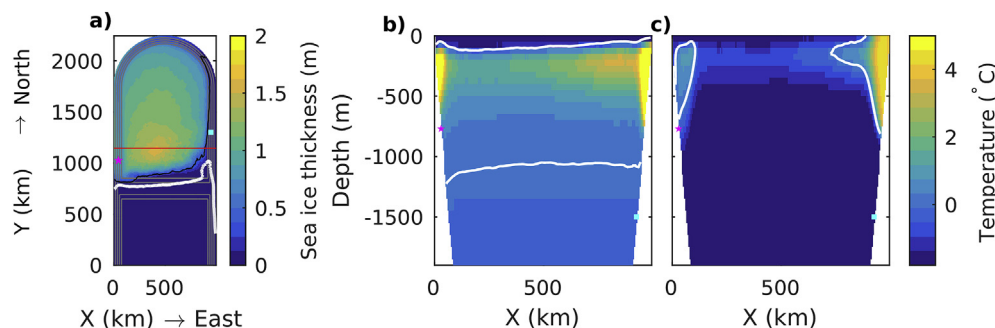
Fig. 4. Model simulation results for FRESH (Stadial-Mode A) (b) Interstadial Experiment (Interstadial-Mode B) (c). Colors show a) sea-ice thickness in Interstadial Experiment and b-c) temperature in the Nordic Seas 400 km north of the Greenland-Scotland Ridge for b) FRESH, c) Interstadial Experiment. Black and white lines in a) mark sea-ice edge (15%) for Interstadial Experiment and FRESH, respectively. Red line marks the transect shown in panels b and c. Gray contours (every 300 m) outline the ocean bathymetry. The 0-temperature-contour is marked in white in panels b and c. Blue square and pink star mark roughly the locations of cores MD99-2284 and GS15-198-36CC.

the 0.25‰/1 °C relationship which is close to linear for this temperature range (Marchitto et al., 2014). Sea level corrections follow the sea level reconstruction curve by Waelbroeck et al., (2002). The core top $\delta^{18}O_{CN}$ from site GS15-198-36CC is used as a modern reference for the downcore sea level corrections. The difference between VPDB and δ_w is corrected for using a constant of 0.3‰. The relative change in δ_w at site MD99-2284 can be explained by:

$$\delta_w = (sealevel(m)*0.0092) - ((Ttop - TDown)*0.23) + 0.3 \qquad (2)$$

where T_{top} is the temperature at core top (or CTD in this case) (-0.38 °C) and T_{down} is the down core temperature in °C as calculated using the Mg/Ca$_{CN}$ calibration on the foraminifera samples. Errors associated with calculation are derived from the analytical error of the isotopes and the errors associated with Mg/Ca$_{CN}$ temperature conversion (supplementary material).

3.3. Chronology

To establish the chronology of core GS15-198-36CC we synchronized the benthic $\delta^{18}O_{CN}$ proxy series based on *C. Neoteretis* to that reconstructed in core MD99-2284 (Dokken et al., 2013) using a Monte Carlo algorithm for proxy-to-proxy stratigraphical alignment (Muschitiello et al., 2015a; 2015b) based on the assumption that changes in bottom-water $\delta^{18}O_{CN}$ at the two sites are virtually synchronous within the resolution of the proxy sampling. The chronology of core MD99-2284 was constructed using one tephra stratigraphic markers identified in Greenland ice cores and tuning of distinct transitions in anhysteretic remnant magnetization (ARM) to changes in NGRIP $\delta^{18}O$ records as detailed in Dokken et al. (2013) and Sadatzki et al. (2019) The alignment algorithm is driven by a Markov Chain Monte Carlo (MCMC) method (Malinverno, 2013) (which was run for 10^6 iterations) and involves nonlinear deformation of the entirety of one record onto a reference record via a Monte Carlo technique that estimates the optimal alignment function accounting for uneven compaction and/or expansion of sediments over time. An account of the mathematical formulation associated with the algorithm is presented in (Muschitiello, 2016). Note that the absolute magnitude and amplitude of variations in benthic $\delta^{18}O_{CN}$ values on both sides of the Nordic Seas basin are comparable (Fig. 2), hence no scaling or detrending was strictly necessary prior to MCMC synchronization. However, to ensure comparability with previous results we followed a standard procedure and pre-normalized the data to be between 0 and 1.

3.4. Model

We modify an existing set-up of the Nordic Seas with the MITgcm (Massachusetts Institute of Technology general circulation model) (Marshall et al., 1997; Losch et al., 2010; Spall, 2011, 2013). The idealized eddy-resolving set-up has two basins; the Nordic Seas and the northern North Atlantic, separated by a ridge with a depth of 1000 m. The two basins have sloping sides and a depth of 2000 m. The sea-surface temperatures are restored toward constant atmospheric temperatures; 10 °C in the south and decreasing gradually to -20 °C at the northern boundary, with a restoring strength of $\Gamma = 40$ W/m^2. The Atlantic Water temperature is set in the southernmost 200 km of the domain, where the full water column is restored toward constant temperatures and a salinity of 35 psμ, with a timescale of one month. The horizontal resolution is 5 km, while there are 30 vertical layers; the upper 20 layers are 50 m and the deeper are 100 m. We use a realistic equation of state and the density is calculated according to the Jackett and McDougall (1995) formula. The vertical diffusivity and viscosity is set to 10^{-5}m^{2}s^{-1} and the diffusivity increases to 1000 m^{2}s^{-1} for unstable conditions to parameterize convection. We use a constant Coriolis parameter of $f = 1.2 \times 10^{-4}$ s^{-1} and advect temperature and salinity using a third-order flux-limiting scheme. The ocean model is coupled to a zero-layer thermodynamic sea ice model with viscous-plastic dynamics (Hibler, 1980; Zhang and Hibler, 1997; Losch et al. 2010). There is no wind forcing, nor precipitation. This choice is motivated by the fact that the model can represent the main circulation of the Nordic Seas only with buoyancy forcing, and produce a sea ice cover in the absence of external forcing. Both the wind and precipitation are two large unknowns during MIS3. In addition, previous studies with a similar setup show that wind forcing has a minor impact on the mean heat exchange between the basins compared to buoyancy forcing (Spall, 2011, 2012).

We perform two experiments. In the first experiment, FRESH, the Atlantic Water temperature in the south is set to 6 °C and freshwater is added to the surface of the Nordic Seas: 0.08 Sv is continuously added to the eastern boundary current north of the Greenland Scotland Ridge (1000–1500 km north, 900–1000 km east). The freshwater input mimics run-off from the Fennoscandian Ice Sheet which mainly occurs during interstadials. The experiment is started from an interstadial-like state with limited sea ice extent and run for 200 years. In the second, Interstadial Experiment, the Atlantic Water temperature in the south is set to 4.5 °C and no external freshwater is added. This experiment is run for 100 years.

4. Results and discussion

4.1. Greenland Stadials

4.1.1. Nordic Seas sea ice cover − preserving North Atlantic water

Proxy reconstructions from GS15-198-36CC and MD99-2284 indicate that the Intermediate water temperature across the Nordic Seas is similar during Greenland Stadials (Fig. 3d). During the Stadials − Mode A, both core sites, in the Denmark Strait and the Faroe-Shetland Channel, experience warm intermediate water of $2.5 \pm 0.5\,^{\circ}C$ as exhibited in the Mg/Ca$_{CN}$ temperature reconstructions (Fig. 3d). Temperatures remain stable (i.e. with small temperature variations) throughout the stadial periods (blue shading in Fig. 3d). This could be a side effect of lower resolution during stadials, compared to interstadials, however the higher resolution in GS15-198-36CC indicate more stability than during interstadials. Nearly identical intermediate water temperatures are recorded in nearby core JM11-F1-19PC for Heinrich Stadial 4 from the same species, *C. neoteretis* (Ezat et al., 2014). The very similar records highlight that the two locations are likely experiencing the same water mass during Heinrich Stadial 4, and potentially during other stadials as well. However, the *M. barleeanum* temperature reconstruction that continues their record to Greenland Stadial 6 (approx. 33.5 ka) do not show the same large amplitudinal differences between Greenland Stadials and Interstadials as seen with the *C. neoteretis* record in MD99-2284. This may be due to a lower sampling frequency in the MD99-2284, or that the samples from JM11-F1-19PC did not undergo reductive cleaning (Ezat et al., 2014) and thereby larger signals are subdued.

The idealized model study by Jensen et al. (2018) shows similar intermediate warming at the eastern and western margins of the Nordic Seas for Stadial − Mode A, fully sea ice covered conditions. With a cold atmosphere, the inflowing Atlantic Water subducts beneath a cold fresh surface layer and sea ice, circulates, and exits the Nordic Seas in the west at the same temperature it entered in the east. The new experiment FRESH has an extensive sea ice cover which extends across the Nordic Seas and southward to the Greenland Scotland Ridge (Fig. 4a, white line). The sea ice is accompanied by a fresh surface layer which is deeper than in the absence of external freshwater input. With external freshwater input, the mean depth of the 34.6 psu isohaline is 750 m, while it is 60 m without the freshwater supply. Similar warm temperatures are found in the east and the west of the Nordic Seas, and the Atlantic Water is found at depths down to 1000 m (Fig. 4b). The combined model results and Mg/Ca$_{CN}$ IWT reconstructions in this study point toward shifts in the stratification and associated sea ice cover regime regulating the across Nordic Seas hydrography during stadial conditions.

Most paleoceanographic records from the Nordic Seas indicate that Greenland Stadials are characterized by extensive near perennial sea ice cover, while Greenland Interstadials are characterized by reduced sea ice cover (Dokken and Jansen, 1999; Gildor and Tziperman, 2003; Rasmussen and Thomsen, 2004; Dokken et al., 2013; Ezat et al., 2014; Sadatzki et al., 2019). The inference that stadial - interstadial changes are related to variations in sea ice cover in the eastern Nordic Seas has recently been supported by sea ice marine biomarker records from the Faroe-Shetland Channel that indicate that Greenland Interstadial periods have reduced sea ice cover in the eastern Nordic Seas (Hoff et al., 2016; Sadatzki et al., 2019) (Fig. 3g and h). Furthermore, climate model experiments over MIS3 D-O intervals performed with the Earth system model LOVECLIM (Menviel et al. 2014), and a fully coupled CCSM3 (Brandefelt et al., 2011) highlight conditions in the North Atlantic and Nordic Seas that are in agreement with sea ice constructions using sea ice biomarkers (Sadatzki et al., 2019) and with other marine proxy data (e.g. Henry et al., 2016). We also note that the prescribed sea ice cover change in the atmospheric model experiment (atmospheric component of Community Climate Model (CCM3)) of (Li et al., 2005) is similar to the reconstruction of Sadatzki et al. (2019).

There are other data interpretations however, that do not support the hypothesis of an extensive sea ice cover during stadials and a reduced sea ice cover during interstadials. Interpretations of dinoflagellate cyst records present an opposing scheme where the eastern Nordic Seas are marked by a homogenous cold upper water column covered by intensive seasonal sea ice formation during the winter and melt during the summer of interstadials (Eynaud et al., 2002; Wary et al., 2015; Wary et al., 2016; Wary et al., 2017a; Wary et al., 2017b). These authors suggest that the dinoflagellate cyst records indicate extensive sea ice in the Nordic Seas associated with Greenland Interstadials and open ocean convection and minimal sea ice associated with Greenland Stadials (Wary et al., 2017b). However, if open ocean convection in the Nordic Seas were to take place during Greenland Stadials, one would expect that the cold air temperatures would cause the salty Atlantic Water to cool and sink to intermediate depths; our data indicate warm temperatures at depth. It is possible that Wary et al. (2015; 2016; 2017a) are instead recording a local polynya that develops over the area, this would align with our results indicating that intermediate water temperatures stay warm ($\approx 2.5\,^{\circ}C$) at both the eastern and western margins, respectively, indicating an insulating sea ice cover across the Nordic Seas during Greenland stadials.

Although there are no published sea ice records from the western Nordic Seas for D-O events, the consistent changes of the intermediate water hydrographic record from MD99-2284 in the Faroe-Shetland Channel (1500 m), and GS15-198-36CC in the Denmark Strait (770 m), may imply the co-occurrence of sea ice production in the two regions (Fig. 3). During the stadials, when sea ice is present in the Norwegian Sea (Fig. 3), the $\delta^{18}O_{CN}$ is light and mirrored in the $\delta^{18}O_{CN}$ of GS15-198-36CC (Fig. 3b). As the age model linking the two cores is formed from the $\delta^{18}O_{CN}$ (see methods) we do not use it as an indicator for the timing and transitions for $\delta^{18}O_{CN}$ between the two sites, but note the markedly similar amplitudes and shape of the records from both sides of the basin. The $\delta^{18}O_{CN}$ amplitude change clearly shows a basin-wide hydrographical adjustment to stadial-interstadial transitions. When the $\delta^{18}O_{CN}$ is heavier the Nordic Seas exhibits interstadial conditions and when it is lighter, stadial conditions. All interstadials have relatively similar oxygen isotopic values around 5.25‰. However, the stadials show increasingly heavier ($\approx 3.5-4.5$‰) $\delta^{18}O_{CN}$ from HS4 toward GS6 (Fig. 3b). We argue that this likely represents a basin wide reflection of increasing global ice volume (Waelbroeck et al., 2002). To further our argument for a pervasive Nordic Seas ice cover we assess the coherent $\delta^{18}O_{CN}$ results in combination with the consistent benthic temperature, and $\delta^{18}O_{NP}$ reconstructions between the cores.

During seasonal sea ice production, sea ice melts in the summer and freshwater is released to the surface. Brine formation takes place in the winter when sea ice grows. Brine formation is the rejection of dense, salty water, where the oxygen isotopic composition of the water mass is retained but becomes more saline (Craig and Gordon, 1965). Brine formation may explain the parallel $\delta^{18}O_{CN}$ depletion during stadials in both planktic and benthic foraminifera (Fig. 3) (Craig and Gordon, 1965; Dokken and Jansen, 1999; Hagen and Hald, 2002). The depletion is rapid and takes place coherently at both the eastern and western margins of the Nordic Seas. If the depletion was mostly forced by temperature changes, we would expect to see a reflection of this as approximately $3-4\,^{\circ}C$ temperature change from interstadial to stadial conditions at both sites (Shackleton, 1974; Marchitto et al., 2014). However, the Mg/Ca$_{CN}$

derived temperature results show changes of only 2 °C (excluding those temperature immediately following HS4 at GS15-198-36CC, to be discussed in section 4.2.2) (Fig. 3). Isotopic composition of ocean water (δ_w) indicates that after global ice volume and temperature have been accounted for that there is both a very similar benthic oxygen isotopic signal between the cores and that there is also a residual oxygen isotope record common for both sites and measured in *C. neoteretis* potentially originating from salinity changes either by brine, or by the movement of various water masses with differing salt content over the core site. Taken at face value the Mg/Ca derived temperature amplitude is insufficient to explain the depleted oxygen isotope values in stadials. Depleted benthic O-isotope values would need to come from freshwater/meltwater which is added at the surface. In order to get such a signal down to 1500 m the most logical mechanism is by sea ice formation and brine expulsion that salinifies and densifies the waters and allows them to sink and mix with the relatively warm intermediate waters.

Another possible explanation for the coherency in $\delta^{18}O_{CN}$ and δ_w signals between sites is that they are simply advected to the Denmark Strait from the Faroe-Shetland Channel due to stronger circulation regime under the sea ice during stadials. Warm intermediate water enters the Nordic Seas in the eastern margin with warm mean temperatures of 2.5 °C (Fig. 3d). This water mass circulates the Nordic Seas and exits in the western margin as an intermediate water mass as part of the DSOW with the same mean temperature (Figs. 3d and 4c). Simulations by Rainsley et al. (2018) seem to support this mechanism.

4.1.2. Additional freshwater drives warm layer deeper

Additional freshwater input to that of sea ice melt during summer alter the stratification. During Greenland stadials, increases in IRD content are recorded at site PS2644-5 and are likely caused by increased iceberg discharge from Greenland, Scandinavia and Iceland (Fig. 3) carried south with the PSW of the East Greenland Current and also appearing in sediment cores south of the sill in the Irminger Sea (van Kreveld et al., 2000; Elliot et al., 2001; Andrews et al., 2017). Contrary to PS2644-5, MD99-2284 shows relatively more IRD present during the interstadials rather than the stadials (Fig. 3f and g). Because most other records from the Faroe-Shetland Channel, Norwegian Sea and North Atlantic support increased IRD and freshwater in the stadials (Dokken and Jansen, 1999; Hall et al., 2011; Barker et al., 2015; Rasmussen et al., 2016; Wary et al., 2017a), we relate this to regional differences in iceberg discharge events (Alvarez-Solas et al., 2018) and motivation for adding freshwater to the numerical model experiment.

The FRESH experiment clarifies the importance of the additional freshwater input to the surface by mimicking freshwater input from the Fennoscandian Ice sheet as either runoff or iceberg discharge. The freshwater input stabilizes the upper water column and allows for sea ice to form even in the presence of inflowing warm Atlantic Water (Jensen, 2017). In the absence of the external freshwater input, the model does not build an extensive sea ice cover in the eastern Nordic Seas for the same Atlantic Water temperature. With no external freshwater input, the Atlantic Water in the Nordic Seas basin is restricted to depths above the sill (1000 m) and mainly follows the boundary of the basin (Jensen et al., 2018). With the additional freshwater, the depth range of the Atlantic Water layer expands, and the heat penetrates deeper. Temperatures above 0 °C are found across the basin (Fig. 4b). Note that this is only true for extensive sea ice conditions, the Atlantic Water is restricted to shallower depths when freshwater is added to experiments without an extensive sea ice cover, or in the absence of external freshwater input (not shown).

The transient evolution of the Nordic Seas temperatures in FRESH shows how the warming deepens with time (Fig. 5). The larger downward diffusion of heat is likely a combination of stronger stratification, higher temperatures at depth, and increased eddy heat fluxes. Stronger stratification in the upper water column due to more freshwater allows for warmer temperatures at depth. The increased vertical temperature contrasts lead to larger vertical heat fluxes due to diffusivity.

Lateral eddy fluxes exchange heat and salt between the baroclinic boundary current and the interior. As sea ice limits heat release to the atmosphere, heat lost by eddy fluxes to the interior explains the small cooling of the boundary current from east to west in FRESH (Fig. 4b). Eddy fluxes increase with increasing temperature and salinity gradients and is hence larger in experiments with external freshwater input, where the density difference between the interior and the boundary current is larger. Spall, (2013) found a balance between diffusion and eddy fluxes in a similar set-up for the Arctic Ocean; increased eddy fluxes are balanced by increased vertical mixing. The increase in eddy heat fluxes in FRESH can therefore account in part for the increased diffusion of heat and the presence of Atlantic Water at greater depths. However, we note that the modeled warming at depth is not as extensive as proxy data suggest. Other mechanisms in addition to diffusion might be required, or the model simulations need to run for a longer time to allow for warmer temperatures at depth. The uncertainties in the temperature reconstructions from the proxy data can explain approximately 1 °C, but there is nevertheless a clear warming signal at depth in the proxy records during all stadials.

In general, both the proxy data and model results show warmer intermediate temperatures during extensive sea ice conditions (stadials). The idealized model simulations suggest that a combination of extensive sea ice and external freshwater input are needed to explain warming below the sill depth (1000 m depth). Note that the freshwater input in the model experiments used here is localized to the eastern Nordic Seas and relatively small, as opposed to the typical hosing experiments where ~1 Sv of freshwater is added to a large part of the North Atlantic (Manabe and Stouffer, 1995; Zhang and Delworth, 2005).

4.2. Greenland Interstadials

4.2.1. Intermediate water mass properties

During Greenland Interstadials (Mode B) the intermediate water temperature reconstructions indicate a similar consistency between the sites as in the stadials, but display larger amplitudinal changes inside the interstadials and markedly lower mean temperatures across the Nordic Seas (Fig. 3d). Mode B has an average intermediate water temperature of 0.6° ± 0.5 °C (Fig. 6e). During Mode B, the eastern margin (MD99-2284) is generally warmer than the western margin (GS15-198-36CC) (Fig. 3d). Mode C is a period that is only clearly visible in Greenland Interstadial 8, immediately following Heinrich Event 4 and may or may not occur during other interstadials. In Mode C, the temperature contrast across the Nordic Seas is reversed; warm temperatures in the Denmark Strait with an average of 4.6° ± 1 °C, and colder in the Faroe-Shetland Channel with an average of 0.3° ± 1 °C (Fig. 6e). Mode C will be discussed separately from the baseline Greenland Interstadial conditions in Section 4.2.2.

During the interstadials, when Greenland is warm (Fig. 3a), the surface and intermediate Atlantic Water in the Nordic Seas is cold (0.6° ± 0.5 °C). Near sea surface temperature records from the eastern North Atlantic indicate that interstadial Atlantic Water temperatures are approximately 6–10 °C (Hall et al., 2011). As Atlantic Water flows across the Iceland - Scotland Ridge it cools by
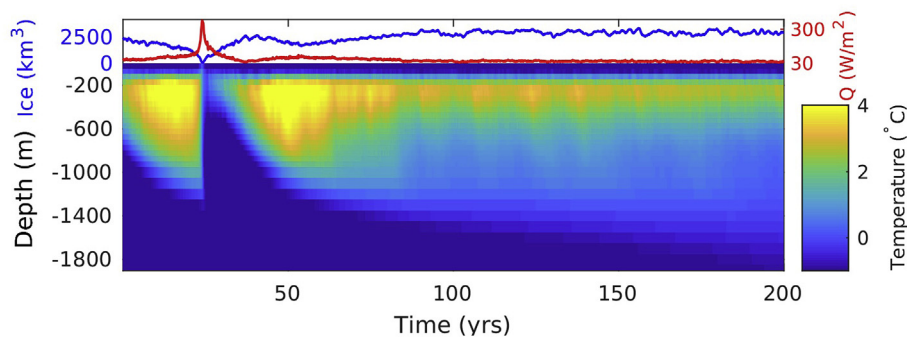
Fig. 5. Colors show temperature averaged over the Nordic Seas (area north of sill) for the FRESH experiment. The blue lines show total sea ice volume (Ice), and the red lines show mean surface heat flux in the Nordic Seas (Q).

heat release to the atmosphere and mixes with other water masses — similar to the modern situation (Mauritzen, 1996; Segtnan et al., 2011; Bosse et al., 2018) — and enters the Nordic Seas with a temperature of approximately 2−4 °C (Fig. 6) (Dokken et al., 2013; Rasmussen and Thomsen, 2014).

In Mode B, as Atlantic Water flows north, it continues to cool through surface fluxes. The biomarker proxies indicate that there is little to no sea ice cover in the eastern Nordic Seas during interstadials (Fig. 3h and i). We propose that the Atlantic Water returns to the North Atlantic in two ways, similar to the modern situation. Atlantic water recirculates in the Nordic Seas and returns to the North Atlantic through the Denmark Strait as an intermediate Atlantic Originating Water (Gascard et al., 1988; Mauritzen and Häkkinen, 1997; Eldevik et al., 2009). In addition, a strong temperature gradient at the air-sea interface during winter results in surface cooling in the Norwegian Sea and vertical mixing that transforms surface Atlantic Water into NSAIW that flows back out the Faroe-Shetland Channel, retaining its saline properties and much of its heat content (Hansen and Østerhus, 2000; Eldevik et al., 2009; Bosse et al., 2018). When the Atlantic water exits the Nordic Seas, it has cooled to a temperature of approximately 0.3 °C (Fig. 6e).

To support this circulation scheme, we look to the benthic $\delta^{13}C_{CN}$. IN general the carbon isotopic signature in foraminiferal calcite is related to ventilation and water mass age (Ravelo and Hillaire-Marcel, 2007; Dokken et al., 2013). For infaunal species, light isotopic pore waters from decomposition of organic matter may add a complication to this situation and the $\delta^{13}C_{CN}$ results need to be treated with caution. *C. neoteretis* is a shallow infaunal species with expected carbon isotopic values slightly more negative than the ambient bottom water composition. However, studies have indicated that the deviation is relatively small for the *Cassidulina* group of benthic foraminifera (e.g. Ishimura et al., 2012), hence we will cautiously use the parameter to infer general changes with respect to water mass aging and ventilation state. When the sea surface is covered by sea ice, surface exchange of CO_2 is inhibited, the sea water ^{13}C decreases due to aging and supply of ^{12}C from gradual decomposition of organic matter. If water becomes trapped in the deep basin of the Nordic Seas due to its density, it will appear older and depleted in $\delta^{13}C$. During interstadials benthic $\delta^{13}C_{CN}$ is depleted compared to stadials at MD99-2284, whereas it is the opposite at the shallower GS15-198-36CC; more enriched during the interstadials than during the stadials. The eastern side of the basin seems to represent a combined signal of Atlantic Water mixing with deeper and older water from the Norwegian Sea. Old water depleted in $\delta^{13}C_{CN}$ mixes irregularly with the warmer Atlantic Water above creating an "unclean" record of the depleted $\delta^{13}C_{CN}$ (Fig. 6f). This produces a mixing gradient across the Nordic

Seas during the interstadial making site GS15-198-36CC better ventilated than site MD99-2284. This is potentially a response to mixing of surface water down to intermediate depths further north or east in the Greenland or Iceland Seas; convecting well ventilated surface water to the depth of GS15-198-36CC. Site GS15-198-36CC always has more enriched $\delta^{13}C_{CN}$ than MD99-2284 because it is a shallower site, despite appearing to always be covered by a permanent sea ice cover or seasonal sea ice cover, formed locally or exported to the site from elsewhere.

The relative abundance of planktic foraminifera species, *N. pachyderma* is commonly used as an indicator of cold, polar water (Bé and Tolderlund, 1971; Jonkers et al., 2010). Based on the data in Fig. 6c we find that the % *N. pachyderma* at the two sites indicates a dominance of *N. pachyderma* at both the eastern and western margins during interstadials. However, at MD99-2284 transfer functions indicate that the near SST (Fig. 6b) is relatively warm (≈3 °C), implying presence of Atlantic species, and thereby Atlantic Water. In the Denmark Strait, the total concentration of *N. pachyderma*, at PS2644-5 has large variations (Fig. 6d) indicative of movement of the sea ice edge (Carstens et al., 1997; Ramseier et al., 2001). Intervals with low absolute abundance suggest a core site that is ice covered with the polar front south and east of the site. Higher planktonic foraminiferal abundance intervals indicate an ice-free or ice-marginal zone where the polar front and sea ice production are close to or north of the core site. At PS2644-5 the concentration of *N. pachyderma* implies that interstadial periods have an ice-free or ice-marginal cover (Fig. 6d). In other words, the Denmark Strait is covered by seasonal ice cover.

To investigate the physical conditions needed to sustain a sea ice-covered Nordic Seas, we examined the Interstadial Model Experiment. As a result of no external freshwater input and warm Atlantic Water, the Interstadial Experiment has a less extensive Nordic Seas ice cover with an ice-free eastern margin (Fig. 4a). There is a fresh surface layer as a result of sea ice melting in the Nordic Seas, but the Atlantic Water inflow is too warm to subduct to depths in the eastern margin (Fig. 4c). While the Atlantic Water is at the surface it prevents sea ice formation. The water loses heat to the atmosphere, and when reaching the northern end of the domain, the surface waters have cooled to the freezing point. As a result, the western boundary is covered in sea ice, and the return flow of Atlantic Water is found at intermediate depths (Fig. 4c). However, the Atlantic Water has cooled substantially and is restricted to depths above the core site. Below 700 m, the model shows cold temperatures across the Nordic Seas.

In support of our results, Zhang et al. (2014b) also find ice free areas in the Nordic Seas during winter conditions in a relatively warm and interstadial-like climate of a CCSM3 MIS3 simulation. The authors explain the ice-free conditions with intense inflow of
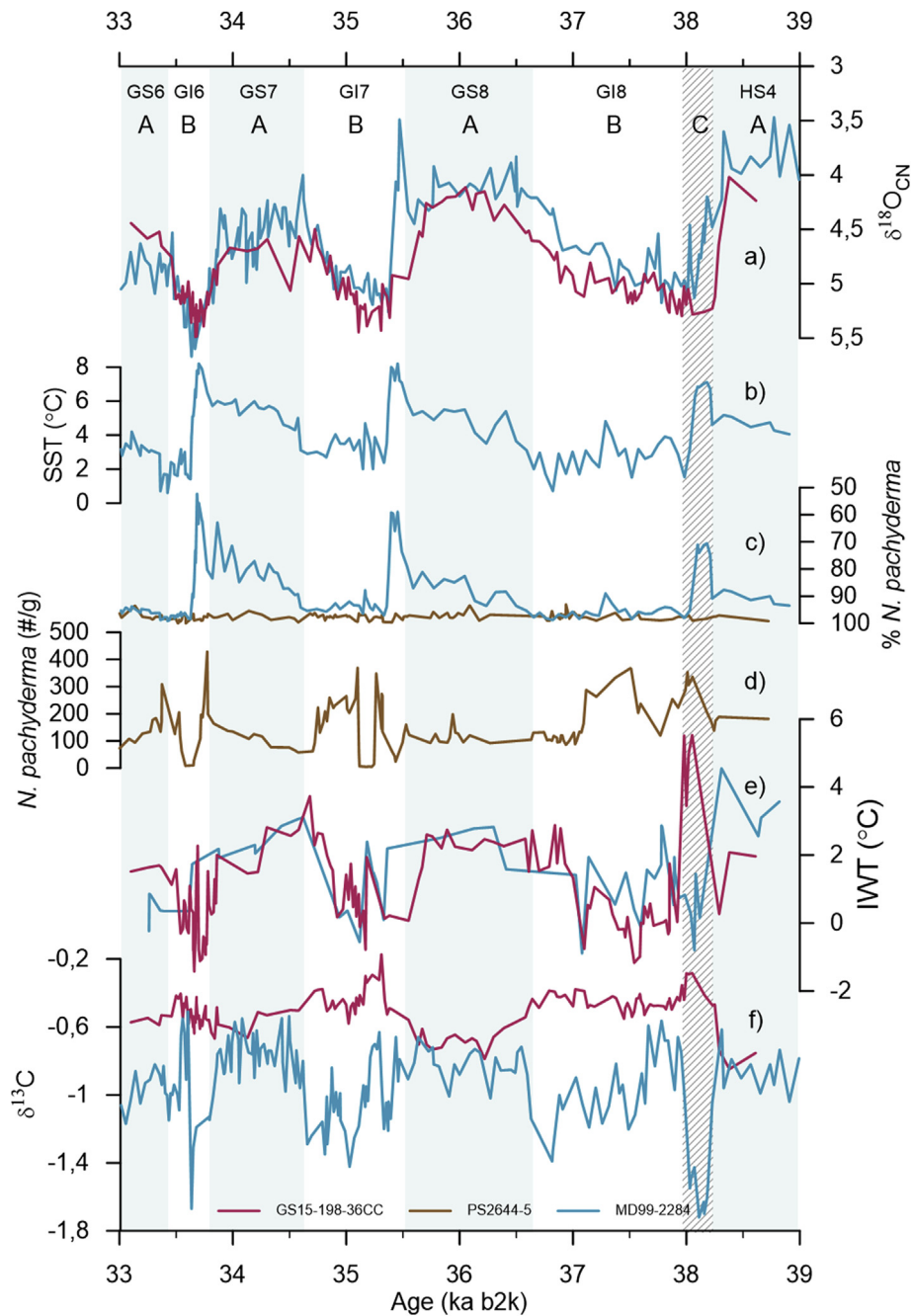
Fig. 6. Downcore proxy records highlighting surface and ventilation changes during the interstadials. a) $\delta^{18}O$ from benthic species C. neoteretis, b) sea surface temperature as calculated using transfer functions on planktonic foraminifera (Dokken et al., 2013), c) % N. pachyderma, d) absolute concentration of N. pachyderma e)Mg/Ca temperature reconstruction of intermediate water from C. neoteretis, and f) $\delta^{13}C$ of benthic C. neoteretis. The colors are blue MD99-2284, pink GS15-198-36CC (Sessford et al., 2018), and brown PS2644-5 (Voelker et al., 2000; Voelker and Haflidason, 2015). Modes A and B correlate with Greenland Stadials and Greenland Interstadials, respectively. Mode C is part of the Greenland Interstadial 8 and indicated with diagonal lines.

Atlantic Water into the Nordic Seas. Menviel et al. (2014) find increased sea-surface salinities in the Nordic Seas during reduced North Atlantic sea ice conditions. The authors do not specify where in the Nordic Seas the salinities increase, but their results argue for the absence of a surface freshwater layer in the Nordic Seas during interstadials.

4.2.2. Nordic Seas mixing

The transient model simulation adds insight to the dynamics of the transition in sea ice and vertical stratification during the DO-

cycles (Fig. 5). The FRESH experiment shows transient unforced changes in sea ice cover and heat content (Fig. 5). Due to the timescale of the oscillation (≈ 30 years), this clearly does not simulate a full D-O cycle. In particular, the time period without a sea ice cover is short. Likely, the model setup does not allow for the mechanisms and feedbacks which keep the area in a sea ice free state. The short time period of the fully sea ice covered state might be related to the domain size. However, despite the short time scale, the model simulation shows what might happen to the water column if the sea ice suddenly disappears. When sea ice rapidly

disappears, the warm intermediate waters are mixed up to the surface. The intermediate waters of the Nordic Seas cool and there is a strong flux of heat from the ocean to the atmosphere (Fig. 5).

The model shows differences in the simulated east and west hydrography during the sea ice free period (not shown). The western side experiences a short time period (≈ 12 months) when the full water column is below $0\,°C$. However, the sea ice quickly grows back in this area and the intermediate waters warm. The eastern margin is dominated by the influence of the Atlantic inflow which increases when the sea ice disappears. Thus, the sea surface is warm ($>0\,°C$) and ice free for a longer time period (≈ 60 months). We propose that this rapid initial response to sea ice disappearance, that is registered in the model simulation, is representative of Mode C. In the proxy record, this is a rapid event that is clearly recorded in Greenland Interstadial 8, immediately following the stadial including Heinrich Event 4, described below as Mode C.

The rapid turnover of the water column, as the sea ice is removed (at the start of the Interstadial), is partially recorded by proxies, and likely a signature of Mode C (Fig. 6). The proxies record a temperature overshoot at the near-surface and temperature drop in intermediate water in the eastern margin at MD99-2284 whereas the western margin records a continuously cold near-surface (high % of N. pachyderma; Fig. 6c), close proximity to the polar front (high # of N. pachyderma; Fig. 6d) and pronounced warming of the intermediate water ($4.6° \pm 1\,°C$; Fig. 6e). (Fig. 6). $\delta^{13}C$ proxy records indicate that water column mixing is different between the eastern and western margins of the Nordic Seas. The isotopic signature of carbon in foraminiferal calcite is related to ventilation and water mass age (Ravelo and Hillaire-Marcel, 2007; Dokken et al., 2013). When the sea surface is covered by sea ice, surface exchange of CO_2 is inhibited, the sea water ^{13}C decreases due to aging and supply of ^{12}C from gradual decomposition of organic matter. When sea ice melts, and deep mixing takes place in the Norwegian Sea, water depleted in $\delta^{13}C$ is mixed up to the surface. The undershoot in depleted $\delta^{13}C_{CN}$ at MD99-2284 may imply that Norwegian Sea Deep Water, containing low $\delta^{13}C$ waters, is mixing upwards with NSAIW in the eastern Nordic Seas to form the outflowing Iceland-Scotland Overflow Water (Hansen and Østerhus, 2000) (Fig. 6), whereas this $\delta^{13}C$ depleted water mass is not present in the shallower core in the western margin (Fig. 6).

The proxy records from the west, in the Denmark Strait, record enrichment in $^{13}C_{CN}$ during interstadials and a consistently cold, surface polar water present throughout both stadials and interstadials (Fig. 6). This indicates that the Denmark Strait does not record the same deep convective instability during interstadials as recorded in the proxy record of the Faroe-Shetland Channel. We propose that the Denmark Strait does not see this deep convective instability for two reasons; sea ice and basin bathymetry. The region is largely still covered by seasonal sea ice, similar to the East Greenland Current in the modern situation. When instability in the water column occurs in the east, together with loss of sea ice, Norwegian Sea Deep Water mixes upwards with the NSAIW giving a negative carbon isotopic anomaly in the feed waters to the overflows into the North Atlantic in the east. The Denmark Strait on the other hand is reflected by intermediate water with high benthic $\delta^{13}C_{CN}$-values apparently without influence of a deeper $\delta^{13}C$ depleted source as in the east. The Iceland Sea basin is shallower than the Norwegian Sea basin. Therefore, DSOW does not come into contact with the deeper, denser, colder water with depleted $\delta^{13}C$ that is recorded at MD99-2284.

A similar deep stratification and water mass aging in the deeper layers was also found for the later MIS3 in the Fram Strait area by Ezat et al. (2019). High resolution radiocarbon measurements from site also support the existence of an older, deep water mass being mixed upwards in interstadials (M. Simon, pers. comm. 2019).

The model results also indicate continuously cold surface waters in the west. However, at the time when sea ice disappears, the central and western parts of the basin have relatively low ($<0\,°C$) temperatures. One reason for the difference between the proxies and the model at the western margin is that the idealized model has a simpler inflow than what occurs in reality. The time period of the homogenous cold waters is short and might not be recorded in the proxy data due to temporal resolution. The intermediate water temperatures in the west warm more quickly than in the east. Another reason might be that the average convection signal in the model is biased by a non-variable sea floor bathymetry and is not capable of separating the basins by their variable depth.

4.3. Summary of stadial/interstadial Nordic Seas circulation

The results from this study indicate that there were two different modes of circulation exchanging water between the North Atlantic and the Nordic Seas during D-O events; Mode A, stadial conditions; and Mode B, baseline interstadial conditions. However, a third event, Mode C is also apparent, taking place at the onset of Greenland Interstadial 8, immediately following Heinrich Event 4 (Fig. 7). Each of these modes results in differing intermediate water properties as reproduced by benthic foraminifera, C. neoteretis.

Mode A has a circulation scheme without extensive vertical mixing or convection in the Nordic Seas, which is fully sea ice-covered (Fig. 7a). However, unlike past studies (Rasmussen and Thomsen, 2004, 2009), the analysis of both the eastern and western margins of the Nordic Seas indicates that overflow waters continue to exit the Nordic Seas at the Greenland-Scotland ridge. In Mode A, intermediate water enters the Nordic Seas in the eastern margin with warm temperatures greater than $4\,°C$ at the near surface (Figs. 6b and 7) (Hall et al., 2011; Dokken et al., 2013). This warm Atlantic Water subducts beneath the sea ice and through advection and eddy fluxes, mixes in the Nordic Seas thereby producing a homogenous water mass down to 1500 m in the Nordic Seas basin. This homogenous water mass has a light benthic $\delta^{18}O_{CN}$ signature. Mode A records the only time during this record that benthic $\delta^{13}C_{CN}$ values at both sides of the basin are similar; approximately $-0.8‰$. This water exits the Nordic Seas, passing over both GS15-198-36CC as Denmark Straight Overflow Water and MD99-2284 as Iceland-Scotland Overflow Water (Fig. 7a) with approximately the same mean temperature $2.5\,°C$ (Fig. 3d). North Atlantic Deep Water in this mode is likely produced by either brine expulsion from seasonal sea ice production in the Nordic Seas, recirculating Southern Ocean Water (Vidal et al., 1998; van Kreveld et al., 2000; Hagen and Hald, 2002) (Fig. 7) and, or, enhanced convection in the sub-polar gyre and does not enter the Nordic Seas.

With a Nordic Seas that has a reduced sea ice cover in the east, Mode B reflects a circulation scheme more similar to modern day (Fig. 7b). At MD99-2284, the near surface Atlantic Water inflow as indicated by transfer functions is cool in comparison to Mode A ($>2\,°C$) and likely extends to the surface, thereby preventing sea ice formation in the east. Mean intermediate water temperatures at both the east and the west margins of the Nordic Seas are $0.6 \pm 0.5\,°C$ and benthic $\delta^{18}O_{CN}$ values are heavy and coherent between sites. However, the sites are not experiencing precisely the same water masses. The benthic $\delta^{13}C_{CN}$ are dissimilar during interstadials with $\delta^{13}C_{CN}$ becoming heavier, and relatively stable (no large fluctuations) in the Denmark Strait and lighter with more fluctuations in the Faroe-Shetland Channel (Fig. 6f). We suggest that this difference arises from the differences in ocean floor bathymetry and convection sites. Both sites experience modified Atlantic Water as intermediate water. However, the Denmark Strait does not record water masses that have experienced vertical
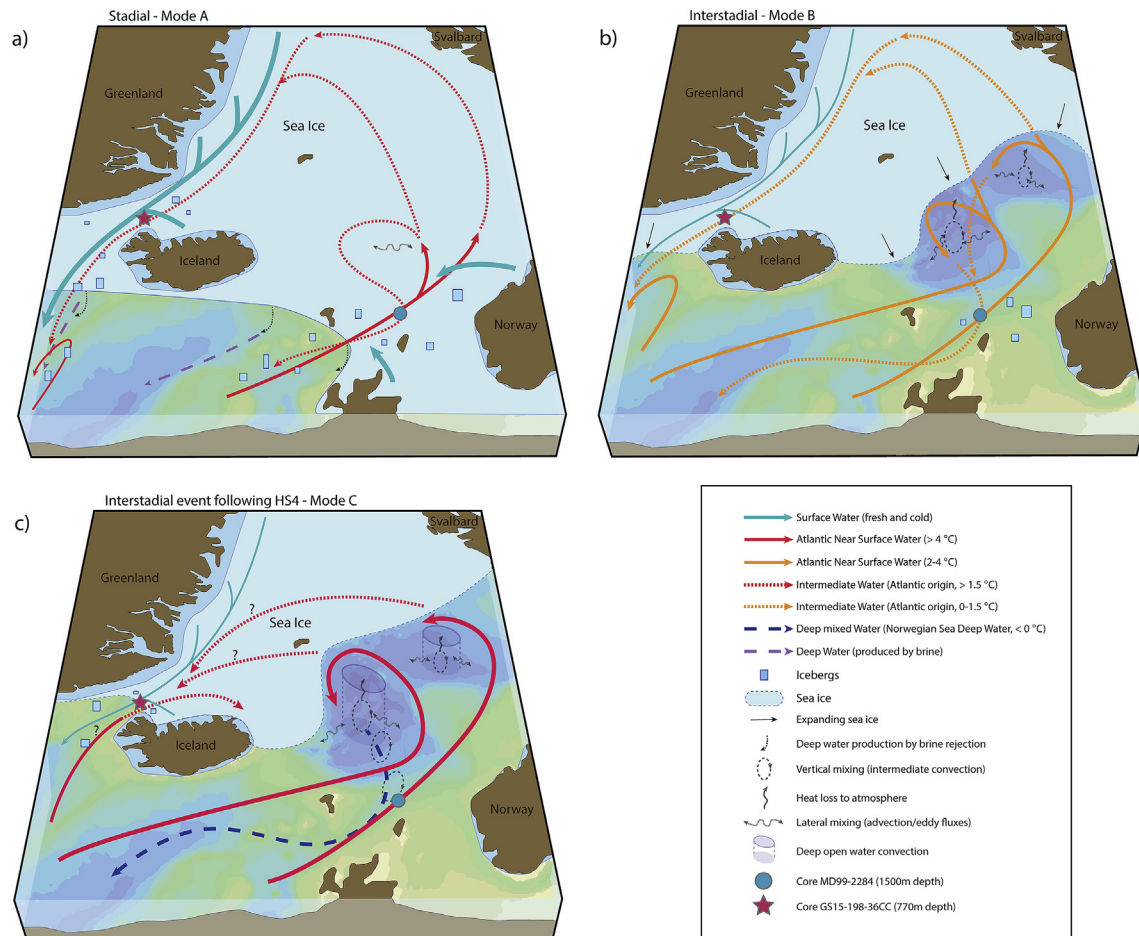
Fig. 7. Schematic illustration of the water masses present in the Nordic Seas across a) Greenland Stadial, Mode A where eddy fluxes and advective mixing produce a homogenous Nordic Seas water column down to at least 1500 m; b) Greenland Interstadial, Mode B where circulation and distribution of water masses are most similar to the modern day situation; and c) Interstadial event following HS4, Mode C where increased warm temperatures at 770 m in the Denmark Strait are a result of either increased inflow of the Northern Icelandic Irminger Current that subduct because of the continued presence of sea ice and fresh water, or recirculated warm water from the eastern Nordic Seas. Interpretations are based on a combination of proxy data, see Table 1, Figs. 3 and 6, and numerical model results discussed in the text.

mixing with intermediate water, but simply recirculated under the sea ice and returned to the North Atlantic via the Denmark Strait. As Atlantic Water moves northward it continues to lose heat to the atmosphere, and when it reaches far enough north it subducts beneath the sea ice and recirculates along the western margin of the basin at intermediate depths (Fig. 7b). Rasmussen and Thomsen (2004) refer to this mode as the end of the sea water transitional cooling phase. This is a period where the cool intermediate waters are gradually warming, and the sea ice edge is gradually moving south and eastward (Fig. 3d, g, h). However, MD99-2284 in the Faroe-Shetland Channel records Atlantic Water that has been vertically mixed with older water masses. This produces a water mass which is similar to what Blindheim and Ådlansvik (1995), refer to as Norwegian Sea Arctic Intermediate Water (NSAIW); an overflow water mass that is produced in the Norwegian and Greenland Seas through vertical mixing and/or on shallow shelf regions through sea ice formation and brine rejection.

The circulation scheme in Mode C is similar to Mode B in that the Nordic Seas has a reduced sea ice cover in the east (Fig. 7). However, it differs in that there is a period of enhanced vertical mixing and water mass transformation. Intermediate water temperatures are markedly warm in the Denmark Strait (4.6 °C), whereas they are colder in the Faroe-Shetland Channel (0.3 °C) (Fig. 3). This difference in temperature indicates that the two water

masses are different. We propose that the combination of the preceding Heinrich Event 4 and a potentially more rapid (than is identified by Sadatzki et al., 2019) retreat of sea ice in the eastern basin following the stadial produces a vigorous overturning with deep convection in the Norwegian Sea, thereby drawing up less ventilated Norwegian Sea Deep Water as indicated by the depleted $\delta^{13}C_{CN}$ ($\approx$ -1.8‰) (Fig. 6f). The temperatures recorded in the benthic data from the Faroe-Shetland Channel are too warm for pure Norwegian Sea Deep Water (Hansen and Østerhus, 2000), indicating that the cold deep water is likely mixing with the warm intermediate water and that the entire water column is affected. However, because of sea floor bathymetry the dense deep waters are unable to enter the Iceland Sea and overflow with the DSOW (Hansen and Østerhus, 2000), instead they are confined to the eastern basin and overflow as Iceland-Scotland Overflow Water. The warm intermediate water temperatures in the Denmark Strait during this initial part of the Interstadial (Mode C) may either be due to a strengthening of the Northern Icelandic Irminger Current because the Atlantic Meridional Overturning Circulation and/or the Atlantic subpolar Gyre is strengthened, or advection from the east of a warm subsurface water mass associated with increased inflow. In both cases the surface waters subducts and flows at depth due to a continued presence of sea ice and a fresh surface layer in the western margin of the Nordic Seas as indicated by the increased

concentration of *N. pachyderma*, and light planktic $\delta^{18}O_{NP}$ (Figs. 6d and 3c). Similar changes in circulation of the Northern Icelandic Irminger Current have been proposed for the Younger Dryas (Rainsley et al., 2018). This results in temperatures ($\approx 5\,°C$) similar to the Atlantic Water temperature range as measured by *C. neoteretis* at 770 m depth (Fig. 6d). The same species contains enriched $\delta^{13}C_{CN}$, indicating that the Denmark Strait is well ventilated (Fig. 6). This circulation mode may be the result of a combination of a strengthened sub-polar gyre, rapid sea ice retreat and a weaker/tilted/erratic jet stream as discussed by Li and Born, (2019).

5. Conclusion

New measurements of intermediate water temperature from the eastern margin of the Nordic Seas show consistent changes with similar measurements from the western margin. Overall, the results indicate similar water mass changes across the Nordic Seas basin during Dansgaard-Oeschger events. Greenland Stadials comprise a Nordic Seas filled with warm Atlantic Water that circulates beneath sea ice and a freshwater layer without losing its Atlantic Water signature as it exits the Denmark Strait. During the Interstadial, weak mixing takes place in the Norwegian Sea with surface waters reaching intermediate depth. Immediately following the Greenland Stadial with Heinrich Event 4 there is evidence for deep mixing in the Norwegian Seas drawing up Norwegian Sea Deep Water. In the Denmark Strait, there is continuous sea ice cover and mixing is too shallow for the deep waters to affect the core site, rather it is under the influence of the Northern Icelandic Irminger Current or inflow of water from the east at intermediate depths. Further studies including high resolution proxy data and additional model simulations are required to assess if this occurs after each stadial event or only following Heinrich events. Widespread sub-surface warming in the Nordic Seas during stadials may have been a crucial mechanism in enhancing thermal erosion of ice streams. Further high-resolution studies into lead-lags between the eastern and western margins of the Nordic Seas for the entire water column hydrography may provide additional insight into mechanisms controlling D-O cycles.

Acknowledgements

Appendix A. Supplementary data

Supplementary data to this article can be found online at https://doi.org/10.1016/j.quascirev.2019.105887.

References

Alvarez-Solas, J., Banderas, R., Robinson, A., Montoya, M., 2018. Oceanic forcing of the Eurasian ice sheet on millennial time scales during the last glacial period. Clim. Past Discuss. 1−27.

Andrews, J.T., Dunhill, G., Vogt, C., Voelker, A.H.L., 2017. Denmark Strait during the late glacial Maximum and marine isotope stage 3: sediment sources and transport processes. Mar. Geol. 390, 181−198.

Barker, S., Greaves, M., Elderfield, H., 2003. A study of cleaning procedures used for foraminiferal Mg/Ca paleothermometry. Geochem. Geophys. Geosyst. 4 (9).

Barker, S., Cacho, I., Benway, H., Tachikawa, K., 2005. Planktonic foraminiferal Mg/Ca as a proxy for past oceanic temperatures: a methodological overview and data compilation for the Last Glacial Maximum. Quat. Sci. Rev. 24 (7−9), 821−834.

Barker, S., Chen, J., Gong, X., Jonkers, L., Knorr, G., Thornalley, D., 2015. Icebergs not the trigger for North Atlantic cold events. Nature 520 (7547), 333−336.

Barrientos, N., Lear, C.H., Jakobsson, M., Stranne, C., O'Regan, M., Cronin, T.M., Gukov, A.Y., Coxall, H.K., 2018. Arctic Ocean benthic foraminifera Mg/Ca ratios and global Mg/Ca-temperature calibrations: new constraints at low temperatures. Geochem. Cosmochim. Acta 236, 240−259.

Bassis, J.N., Petersen, S.V., Mac Cathles, L., 2017. Heinrich events triggered by ocean forcing and modulated by isostatic adjustment. Nature 542 (7641), 332−334.

Bé, A.W.H., Tolderlund, D.S., 1971. Distribution and ecology of living planktonic foraminifera in surface waters of the Atlantic and Indian oceans. In: The Micropaleontology of Oceans. Cambridge University Press, Cambridge, pp. 105−149.

Blindheim, J., Ådlandsvik, B., 1995. Episodic formation of intermediate water along the Greenland Sea Arctic front. ICES CM 1995/Mini 6 (11).

Boyle, E.A., 1983. Manganese carbonate overgrowths on foraminifera tests. Geochem. Cosmochim. Acta 47, 1815−1819.

Boyle, E.A., Keigwin, L.D., 1985/86. Comparison of Atlantic and Pacific paleochemical records for the last 215,000 years: changes in deep ocean circulation and chemical inventories. Earth Planet. Sci. Lett. 76, 135−150.

Brandefelt, J., Kjellström, E., Näslund, J.O., Strandberg, G., Voelker, A.H.L., Wohlfarth, B., 2011. A coupled climate model simulation of Marine Isotope Stage 3 stadial climate. Clim. Past 7 (2), 649−670.

Broecker, W.S., Peteet, D.M., Rind, D., 1985. Does the ocean-atmosphere system have more than one stable mode of operation? Nature 315, 21−26.

Buizert, C., et al., 2015. Precise interpolar phasing of abrupt climate change during the last ice age. Nature 520, 661.

Carstens, J., Hebbeln, D., Wefer, G., 1997. Distribution of planktic foraminifera at the ice margin in the Arctic (Fram Strait). Mar. Micropaleontol. 29 (3), 257−269.

Craig, H., Gordon, L.I., T. E, 1965. Deuterium and oxygen 18 variations in the ocean and the marine atmosphere. In: Stable Isotopes in Oceanographic Studies and Paleotemperatures, pp. 9−130 (V. Lishi e F., Pisa, Spoleto, Italy).

Dansgaard, W., et al., 1993. Evidence for general instability of past climate from a 250-kyr ice-core record. Nature 364, 218−220.

Darling, K.F., Kucera, M., Kroon, D., Wade, C.M., 2006. A resolution for the coiling direction paradox in Neogloboquadrina pachyderma. Paleoceanography 21 (2).

Dokken, T., Jansen, E., 1999. Rapid changes in the mechanism of ocean convection during the last glacial period. Nature 401, 458−461.

Dokken, T.M., Nisancioglu, K.H., Li, C., Battisti, D.S., Kissel, C., 2013. Dansgaard-Oeschger cycles: interactions between ocean and sea ice intrinsic to the Nordic seas. Paleoceanography 28 (3), 491−502.

Eldevik, T., Nilsen, J.E.Ø., Iovino, D., Anders Olsson, K., Sandø, A.B., Drange, H., 2009. Observed sources and variability of Nordic seas overflow. Nat. Geosci. 2 (6), 406−410.

Elliot, M., Labeyrie, L., Dokken, T., Manthé, S., 2001. Coherent patterns of ice-rafted debris deposits in the Nordic regions during the last glacial (10-60 ka). Earth Planet. Sci. Lett. 194, 151−163.

Eynaud, F., Turon, J.L., Matthiessen, J., Kissel, C., Peypouquet, J.P., Vernal, A.d., Henry, M., 2002. Norwegian sea-surface palaeoenvironments of marine oxygen-isotope stage 3: the paradoxical response of dinoflagellate cysts. J. Quat. Sci. 17 (4), 349−359.

Eynaud, F., Cronin, T.M., Smith, S.A., Zaragosi, S., Mavel, J., Mary, Y., Mas, V., Pujol, C., 2009. Morphological variability of the planktonic foraminifer Neogloboquadrina pachyderma from ACEX cores: implications for late Pleistocene circulation in the Arctic Ocean. Micropaleontology 55 (2/3), 101−116.

Ezat, M.M., Rasmussen, T.L., Groeneveld, J., 2014. Persistent intermediate water warming during cold stadials in the southeastern Nordic seas during the past 65 k.y. Geology 42 (8), 663−666.

Ezat, M.M., Rasmussen, T.L., Skinner, L.C., Zamelczyk, K., 2019. Deep ocean 14C ventilation age reconstructions from the Arctic Mediterranean reassessed. Earth Planet. Sci. Lett. 518, 67−75. https://doi.org/10.1016/j.epsl.2019.04.027.

Ferguson, J.E., Henderson, G.M., Kucera, M., Rickaby, R.E.M., 2008. Systematic change of foraminiferal Mg/Ca ratios across a strong salinity gradient. Earth Planet. Sci. Lett. 265 (1−2), 153−166.

updated daily Fetterer, F., Knowles, K., Meier, W., Savoie, M., Windnagel, A.K., 2017. Sea Ice Index, Version 3. Boulder, Colorado USA. https://doi.org/10.7265/N5K072F8. (Accessed 25 October 2018).

Gascard, J.-C., Kergomard, C., Jeannin, P.-F., Fily, M., 1988. Diagnostic study of the Fram Strait marginal ice zone during summer from 1983 and 1984 marginal ice zone experiment Lagrangian observations. J. Geophys. Res.: Oceans 93 (C4), 3613−3641.

Gildor, H., Tziperman, E., 2003. Sea ice switches and abrupt climate change. Philos. Trans. R. Soc. London, Ser. A 36 (1810), 1935−1944.

Greaves, M., et al., 2008. Interlaboratory comparison study of calibration standards for foraminiferal Mg/Ca thermometry. Geochem. Geophys. Geosyst. 9 (8).

Hagen, S., Hald, M., 2002. Variation in surface and deep-water circulation in the Denmark Strait, North Atlantic, during marine isotope stages 3 and 2. Paleoceanography 17 (4), 13-11-13-16.

Hall, I.R., Colmenero-Hidalgo, E., Zahn, R., Peck, V.L., Hemming, S.R., 2011. Centennial- to millennial-scale ice-ocean interactions in the subpolar northeast Atlantic 18-41 kyr ago. Paleoceanography 26 (2) (n/a-n/a).

Hansen, B., Østerhus, S., 2000. North Atlantic-nordic seas exchanges. Prog. Oceanogr. 45, 109−208.

Hasenfratz, A.P., Martínez-García, A., Jaccard, S.L., Vance, D., Wälle, M., Greaves, M., Haug, G.H., 2017. Determination of the Mg/Mn ratio in foraminiferal coatings:

an approach to correct Mg/Ca temperatures for Mn-rich contaminant phases. Earth Planet. Sci. Lett. 457, 335–347.

Henry, L.G., McManus, J.F., Curry, W.B., Roberts, N.L., Piotrowski, A.M., Keigwin, L.D., 2016. North Atlantic Ocean circulation and abrupt climate change during the last glaciation. Science 353 (6298), 470–474.

Hibler III, W.D., 1980. Modeling a variable thickness sea ice cover. Mon. Weather Rev. 108, 1943–1973.

Hoff, U., Rasmussen, T.L., Stein, R., Ezat, M.M., Fahl, K., 2016. Sea ice and millennial-scale climate variability in the Nordic seas 90 kyr ago to present. Nat. Commun. 7, 12247.

Hönisch, B., Allen, K.A., Lea, D.W., Spero, H.J., Eggins, S.M., Arbuszewski, J., deMenocal, P., Rosenthal, Y., Russell, A.D., Elderfield, H., 2013. The influence of salinity on Mg/Ca in planktic foraminifers - evidence from cultures, core-top sediments and complementary d18O. Geochem. Cosmochim. Acta 121, 196–213.

Ishimura, T., Tsunogai, U., Hasegawa, S., Nakagawa, F., Oi, T., Kitazato, H., Suga, H., Toyofuku, T., 2012. Variation in stable carbon and oxygen isotopes of individual benthic foraminifera: tracers for quantifying the magnitude of isotopic disequilibrium. Biogeosciences 9, 4353–4367. https://doi.org/10.5194/bg-9-4353-2012.

Jackett, D.R., McDougall, T.J., 1995. Minimal adjustment of hydrographic profiles to achieve static stability. J. Atmos. Ocean. Technol. 12, 381–389. https://doi.org/10.1175/1520-0426(1995)012,0381:MAOHPT.2.0.CO;2.

Jeansson, E., Jutterström, S., Rudels, B., Anderson, L.G., Anders Olsson, K., Jones, E.P., Smethie, W.M., Swift, J.H., 2008. Sources to the east Greenland current and its contribution to the Denmark Strait Overflow. Prog. Oceanogr. 78 (1), 12–28.

Jensen, M.F., 2017. Abrupt Changes in Sea Ice and Dynamics of Dansgaard-Oeschger Events. The University of Bergen, Bergen.

Jensen, M.F., Nisancioglu, K.H., Spall, M.A., 2018. Large changes in sea ice triggered by small changes in Atlantic water temperature. J. Clim. 0 (0) null.

Johnsen, S.J., Dahl-Jensen, D., Gundestrup, N., Steffensen, J.P., Clausen, H.B., Miller, H., Masson-Delmotte, V., Sveinbjörnsdottir, A.E., White, J., 2001. Oxygen isotope and palaeotemperature records from six Greenland ice-core stations: camp Century, Dye-3, GRIP, GISP2, Renland and NorthGRIP. J. Quat. Sci. 16 (4), 299–307.

Jonkers, L., Moros, M., Prins, M.A., Dokken, T., Dahl, C.A., Dijkstra, N., Perner, K., Brummer, G.-J.A., 2010. A reconstruction of sea surface warming in the northern North Atlantic during MIS 3 ice-rafting events. Quat. Sci. Rev. 29 (15–16), 1791–1800.

Kleppin, H., Jochum, M., Otto-Bliesner, B., Shields, C.A., Yeager, S., 2015. Stochastic atmospheric forcing as a cause of Greenland climate transitions. J. Clim. 28 (19), 7741–7763.

Krebs, U., Timmermann, A., 2007. Tropical air–sea interactions accelerate the recovery of the Atlantic meridional overturning circulation after a major shutdown. J. Clim. 20 (19), 4940–4956.

Kristjánsdóttir, G.B., Lea, D.W., Jennings, A.E., Pak, D.K., Belanger, C., 2007. New spatial Mg/Ca-temperature calibrations for three Arctic, benthic foraminifera and reconstruction of north Iceland shelf temperature for the past 4000 years. Geochem. Geophys. Geosyst. 8 (3).

Li, C., Born, A., 2019. Coupled atmosphere-ice-ocean dynamics in Dansgaard-Oeschger events. Quat. Sci. Rev. 203, 1–20.

Li, C., Battisti, D.S., Bitz, C.M., 2010. Can North Atlantic sea ice anomalies account for Dansgaard–Oeschger climate signals? J. Clim. 23 (20), 5457–5475.

Li, C., Battisti, D.S., Schrag, D.P., Tziperman, E., 2005. Abrupt climate shifts in Greenland due to displacements of the sea ice edge. Geophys. Res. Lett. 32 (19) (n/a-n/a).

Losch, M., Menemenlis, D., Campin, J.M., Heimbach, P., Hill, C., 2010. On the formulation of sea-ice models. Part 1: effects of different solver implementations and parameterizations. Ocean Model. 33, 129–144.

Maffezzoli, N., Vallelonga, P., Edwards, R., Saiz-Lopez, A., Turetta, C., Kjær, H.A., Barbante, C., Vinther, B., Spolaor, A., 2018. 120,000 year record of sea ice in the North Atlantic. Clim. Past Discuss. 1–19.

Malinverno, A., 2013. Data report: Monte Carlo correlation of sediment records from core and downhole log measurements at Sites U1337 and U1338 (IODP Expedition 321). H. Pälike, H. Lyle, H. Nishi, I. Raffi, K. Gamage and A. Klaus. Exped. 320, 321.

Manabe, S., Stouffer, R.J., 1995. Simulation of abrupt climate change induced by freshwater input to the North Atlantic Ocean. Nature 378, 165.

Marchitto, T.M., Curry, W.B., Lynch-Stieglitz, J., Bryan, S.P., Cobb, K.M., Lund, D.C., 2014. Improved oxygen isotope temperature calibrations for cosmopolitan benthic foraminifera. Geochem. Cosmochim. Acta 130, 1–11.

Marcott, S.A., et al., 2011. Ice-shelf collapse from subsurface warming as a trigger for Heinrich events. Proc. Natl. Acad. Sci. U. S. A. 108 (33), 13415–13419.

Marshall, J., Hill, C., Perelman, L., Adcroft, A., 1997. Hydrostatic, quasi-hydrostatic, and non-hydrostatic ocean modeling. J. Geophys. Res. 102, 5733–65752.

Masson-Delmotte, V., et al., 2013. Information from paleoclimate archives. In: Stocker, T.F., Qin, D., Plattner, G.-K., Tignor, M., Allen, S.K., Boschung, J., Nauels, A., Xia, Y., Bex, V., Midgley, P.M. (Eds.), Climate Change 2013: the Physical Science Basis. Contribution to Working Group I in the Fifth Assessment Report of the Intergovernmental Panel on Climate Change. Cambridge University Press, Cambridge UK and New York, NY, USA.

Mauritzen, C., 1996. Production of dense overflow waters feeding the North Atlantic across the Greenland-Scotland Ridge. Part 1: evidence for a revised circulation scheme. Deep Sea Res. Oceanogr. Res. Pap. 43 (6), 769–806.

Mauritzen, C., Häkkinen, S., 1997. Influence of sea ice on the thermohaline circulation in the Arctic-North Atlantic Ocean. Geophys. Res. Lett. 24 (24), 3257–3260.

Menviel, L., Timmermann, A., Friedrich, T., England, M.H., 2014. Hindcasting the continuum of Dansgaard-Oeschger variability: mechanisms, patterns and timing. Clim. Past 10 (1), 63–77.

Muschitiello, F., 2016. Deglacial Impact of the Scandinavian Ice Sheet on the North Atlantic Climate System. Stockholm University.

Muschitiello, F., Andersson, A. Wohlfarth, B., Smittenberg, R.H., 2015a. The C20 highly branched isoprenoid biomarker - a new diatom-sourced proxy for summer trophic conditions? Org. Geochem. 81, 27–33.

Muschitiello, F., Pausata, F.S.R., Watson, J.E., Smittenberg, R.H., Salih, A.A.M., Brooks, S.J., Whitehouse, N.J., Karlatou-Charalampopoulou, A., Wohlfarth, B., 2015b. Fennoscandian freshwater control on Greenland hydroclimate shifts at the onset of the Younger Dryas. Nat. Commun. 6 (8939).

Olsen, A., et al., 2016. The Global Ocean Data Analysis Project version 2 (GLODAPv2) — an internally consistent data product for the world ocean. Earth Syst. Sci. Data 8 (2), 297–323.

Pena, L.D., Cacho, I., Calvo, E., Pelejero, C., Eggins, S., Sadekov, A., 2008. Characterization of contaminant phases in foraminifera carbonates by electron microprobe mapping. Geochem. Geophys. Geosyst. 9 (7).

Petersen, S.V., Schrag, D.P., Clark, P.U., 2013. A new mechanism for Dansgaard-Oeschger cycles. Paleoceanography 28 (1), 24–30.

Rahmstorf, S., 2002. Ocean circulation and climate during the past 120,000 years. Nature 419, 207–214.

Rainsley, E., Menviel, L., Fogwill, C.J., Turney, C.S.M., Hughes, A.L.C., Rood, D.H., 2018. Greenland ice mass loss during the younger Dryas driven by Atlantic meridional overturning circulation feedbacks. Sci. Rep. 8 (1).

Ramseier, R.O., Garrity, C., Martin, T., 2001. An overview of sea-ice conditions in the Greenland Sea and the relationship of oceanic sedimentation to the ice regime. In: Schäfer, P., Ritzrau, W., Schlüter, M., Thiede, J. (Eds.), The Northern North Atlantic. Springer Link, Berlin, pp. 19–38.

Rasmussen, T.L., Thomsen, E., 2004. The role of the North Atlantic Drift in the millennial timescale glacial climate fluctuations. Palaeogeogr. Palaeoclimatol. Palaeoecol. 210 (1), 101–116.

Rasmussen, T.L., Thomsen, E., 2009. Ventilation changes in intermediate water on millennial time scales in the SE Nordic seas, 65-14 kyr BP. Geophys. Res. Lett. 36 (1).

Rasmussen, T.L., Thomsen, E., 2014. Brine formation in relation to climate changes and ice retreat during the last 15,000 years in Storfjorden, Svalbard, 76-78°N. Paleoceanography 29 (10), 911–929.

Rasmussen, T.L., Thomsen, E., Moros, M., 2016. North Atlantic warming during Dansgaard-Oeschger events synchronous with Antarctic warming and out-of-phase with Greenland climate. Sci. Rep. 6, 20535.

Ravelo, A.C., Hillaire-Marcel, C., 2007. Chapter Eighteen: the Use of Oxygen and Carbon Isotopes of Foraminifera in Paleoceanography, vol. 1, pp. 735–764.

Rosenthal, Y., Field, M.P., Sherrell, R.M., 1999. Precise determination of element/calcium ratios in calcareous samples using sector field inductively coupled plasma mass spectrometry. Anal. Chem. 71 (15), 3248–3253.

Rudels, B., Quadfasel, D., 1991. The Arctic Ocean component in the Greenland-Scotland overflow. ICES CM 1991/C 30, 1–21.

Sadatzki, H., Dokken, T., Berben, S.M.P., Muschitiello, F., Stein, R., Fahl, K., Menviel, L., Timmermann, A., Jansen, E., 2019. Sea ice variability in the southern Norwegian Sea during glacial Dansgaard-Oeschger climate cycles. Sci. Adv. 5 (3).

Sarnthein, M., Winn, K., Jung, S.J.A., Duplessy, J.-C., Labeyrie, L., Erlenkeuser, H., Ganssen, G., 1994. Changes in east Atlantic deepwater circulation over the last 30,000 years: eight time slice reconstructions. Paleoceanography 9 (2), 209–267.

Schlitzer, R., 2014. Ocean Data View.

Segtnan, O.H., Furevik, T., Jenkins, A.D., 2011. Heat and freshwater budgets of the Nordic seas computed from atmospheric reanalysis and ocean observations. J. Geophys. Res.: Oceans 116 (C11).

Sessford, E.G., Tisserand, A.A., Risebrobakken, B., Andersson, C., Dokken, T., Jansen, E., 2018. High-resolution benthic Mg/Ca temperature record of the intermediate water in the Denmark strait across D-O stadial-interstadial cycles. Paleoceanogr. Paleoclim. 33 (11), 1169–1185.

Shackleton, N.J., 1974. Attainment of Isotopic Equilibrium between Ocean Water and the Benthonic Foraminifera Genus Uvigerina: Isotopic Changes in the Ocean during the Last Glacial, vol. 219. Colloques Internationaux du C.N.R.S, pp. 203–209.

Shaffer, G., Olsen, S.M., Bjerrum, C.J., 2004. Ocean subsurface warming as a mechanism for coupling Dansgaard-Oeschger climate cycles and ice-rafting events. Geophys. Res. Lett. 31 (24).

Skirbekk, K., Hald, M., Marchitto, T.M., Junttila, J., Kristensen, D.K., Sørensen, S.A., 2016. Benthic foraminiferal growth seasons implied from Mg/Ca-temperature correlations for three Arctic species. Geochem. Geophys. Geosyst. 17 (11), 4684–4704.

Spall, M.A., 2011. On the role of eddies and surface forcing in the heat transport and overturning circulation in marginal sea. J. Mar. Res. 24, 4844–4858.

Spall, M.A., 2012. Influences of precipitation on water mass transformation and deep convection. J. Phys. Oceanogr. 42, 1684–1699.

Spall, M.A., 2013. On the circulation of Atlantic water in the Arctic Ocean. J. Phys. Oceanogr. 43, 2352–2371.

Tanhua, T., Olsson, K.A., Jeansson, E., 2005. Formation of Denmark Strait overflow water and its hydro-chemical composition. J. Mar. Syst. 57 (3–4), 264–288.

Ullgren, J.E., Darelius, E., Fer, I., 2016. Volume transport and mixing of the Faroe

Bank Channel overflow from one year of moored measurements. Ocean Sci. 12 (2), 451—470.

Våge, K., Pickart, R.S., Spall, M.A., Valdimarsson, H., Jónsson, S., Torres, D.J., Østerhus, S., Eldevik, T., 2011. Significant role of the North Icelandic Jet in the formation of Denmark Strait overflow water. Nat. Geosci. 4 (10), 723—727.

Våge, K., Pickart, R.S., Spall, M.A., Moore, G.W.K., Valdimarsson, H., Torres, D.J., Erofeeva, S.Y., Nilsen, J.E.Ø., 2013. Revised circulation scheme north of the Denmark Strait. Deep Sea Res. Oceanogr. Res. Pap. 79, 20—39.

van Kreveld, S., Sarnthein, M., Erlenkeuser, H., Grootes, P., Jung, S., Nadeau, M.J., Pflaumann, U., Voelker, A., 2000. Potential links between surging ice sheets, circulation changes, and the Dansgaard-Oeschger Cycles in the Irminger Sea, 60-18 Kyr. Paleoceanography 15 (4), 425—442.

Vidal, L., Labeyrie, L., Weering, T.C.E., 1998. Benthic δ18O records in the north Atlantic over the last glacial period (60—10 kyr): evidence for brine formation. Paleoceanography 13 (3), 245—251.

Voelker, A., 2002. Global distribution of centennial-scale records for Marine Isotope Stag (MIS) 3: a database. Quat. Sci. Rev. 21, 1185—1212.

Voelker, A., Grootes, P., Nadeau, M.J., Sarnthein, M., 2000. Radiocarbon levels in the Iceland Sea from 25-53 kyr and their link to the Earth's magnetic field intensity. Radiocarbon 42 (3), 437—452.

Voelker, A.H.L., Haflidason, H., 2015. Refining the Icelandic tephrachronology of the last glacial period — the deep-sea core PS2644 record from the southern Greenland Sea. Glob. Planet. Chang. 131, 35—62.

Voelker, A.H.L., Sarnthein, M., Grootes, P.M., Erlenkeuser, H., Laj, C., Mazaud, A., Nadeau, M.-J., Schleicher, M., 1998. Correlation of marine 14C ages from the Nordic seas with the GISP2 isotope record: implications for 14C calibration beyond 25 ka BP. Radiocarbon 40 (01), 517—534.

Waelbroeck, C., Labeyrie, L., Michel, E., Duplessy, J.C., McManus, J.F., Lambeck, K., Balbon, E., Labracherie, M., 2002. Sea-level and deep-water temperature changes derived from benthic foraminifera isotopic records. Quat. Sci. Rev. 21 (1—3), 295—305.

Wang, Y.J., Cheng, H., Edwards, R.L., An, Z.S., Wu, J.Y., Shen, C.-C., Dorale, J.A., 2001. A high-resolution absolute-dated Late Pleistocene monsoon record from Hulu Cave, China. Science 294, 2345—2348.

Wary, M., Eynaud, F., Rossignol, L., Zaragosi, S., Sabine, M., Castera, M.-H., Billy, I., 2017a. The southern Norwegian Sea during the last 45 ka: hydrographical re-organizations under changing ice-sheet dynamics. J. Quat. Sci. 32 (7), 908—922.

Wary, M., Eynaud, F., Rossignol, L., Lapuyade, J., Gasparotto, M.-C., Londeix, L., Malaizé, B., Castéra, M., Charlier, K., 2016. Norwegian Sea warm pulses during Dansgaard-Oeschger stadials: zooming in on these anomalies over the 35—41 ka cal BP interval and their impacts on proximal European ice-sheet dynamics. Quat. Sci. Rev. 151, 255—272.

Wary, M., Eynaud, F., Swingedouw, D., Masson-Delmotte, V., Matthiessen, J., Kissel, C., Zumaque, J., Rossignol, L., Jouzel, J., 2017b. Regional seesaw between the North Atlantic and Nordic Seas during the last glacial abrupt climate events. Clim. Past 13 (6), 729—739.

Wary, M., et al., 2015. Stratification of surface waters during the last glacial millennial climatic events: a key factor in subsurface and deep-water mass dynamics. Clim. Past Discuss. 11 (3), 2077—2119.

Zhang, J., Hibler III, W.D., 1997. On an efficient numerical method for modeling sea ice dynamics. J. Geophys. Res. 102, 8691—8702. https://doi.org/10.1029/96JC03744.

Zhang, R., Delworth, T.L., 2005. Simulated tropical response to a substantial weakening of the Atlantic Thermohaline Circulation. J. Clim. 18, 1853—1860.

Zhang, X., Lohmann, G., Knorr, G., Purcell, C., 2014a. Abrupt glacial climate shifts controlled by ice sheet changes. Nature 512, 290.

Zhang, X., Prange, M., Merkel, U., Schulz, M., 2014b. Instability of the Atlantic overturning circulation during marine isotope stage 3. Geophys. Res. Lett. 41, 4285—4293. https://doi.org/10.1002/2014GL060321.

Zhang, X., Prange, M., Merkel, U., Schulz, M., 2015. Spatial fingerprint and magnitude of changes in the Atlantic meridional overturning circulation during marine isotope stage 3. Geophys. Res. Lett. 42 (6), 1903—1911.

Zhang, X., Knorr, G., Lohmann, G., Barker, S., 2017. Abrupt North Atlantic circulation changes in response to gradual CO2 forcing in a glacial climate state. Nat. Geosci. 10, 518.